

Random Nonlinear Dynamics of a Spur Gear Pair by Path Integration

by

©Yubing Wen

A Thesis submitted to the
School of Graduate Studies
in partial fulfillment of the
requirements for the degree of
Master of Engineering

**Faculty of Engineering and Applied Science
Memorial University of Newfoundland
October, 2014**

St. John's

Newfoundland

Abstract

The research investigates the random nonlinear vibration of a spur gear pair subjected to both deterministic and random loads by path integration method. Different models and approaches to apply the path integration method are presented in Chapters 2–4. Backlash nonlinearity and time-varying mesh stiffness in gear systems are both considered in Chapters 2 and 3. In Chapter 2, the time-varying mesh stiffness is modeled as a constant plus a cosinusoidal component, and the discontinuous backlash nonlinearity is approximated with a cubic polynomial through curve fitting. Then Gaussian closure procedure is employed to obtain the mean and variance of transition probability density function (PDF). In Chapter 3, the time-varying mesh stiffness is approximated with a square wave function. The variance of the responses is calculated and expressed as closed forms for two different cases in gear systems. In Chapter 4, the gear rattling model which only considers backlash is presented. A degenerate Gaussian distribution is employed as transition PDF. The path integration results are compared with deterministic results (Chapters 2 and 3) and Monte Carlo simulation results (Chapters 3 and 4). Good agreement is found between them, which could verify the accuracy of path integration method in the study of random gear dynamics.

Acknowledgments

I would like to express my sincere gratitude to my supervisor Dr. James Yang. With his encouragement, guidance and support during coursework, research, paper and thesis writing, I could successfully conduct my research and enhance analytical skills. Appreciation is also made to the Faculty of Engineering and Applied Science in particular the graduate office. With the effort from faculty, staff and students, I could devote myself to a dynamic and innovative research environment. Acknowledgment is made to the financial support from School of Graduate Studies and Research & Development Corporation of Newfoundland and Labrador.

I would also like to express my sincere gratitude to my Mom, Dad and my family for their support, concern and encouragement from both physical and mental aspects. Without their support, I could not further my academic studies. I would also like to thank my friend Hongyuan Qiu for his help with both coursework and research. Thanks are also extended to my friends for their encouragement and shared experience during my graduate studies.

Table of Contents

Abstract	ii
Acknowledgments	iii
Table of Contents	vi
List of Tables	vii
List of Figures	ix
1 Introduction	1
1.1 Scope of the Research	1
1.2 Thesis Outline	2
1.3 Literature Review	3
1.3.1 Linear Gear Dynamics	3
1.3.2 Nonlinear Gear Dynamics	4
1.3.3 Stochastic Gear Dynamics	7
1.3.4 Summary of previous work	9
1.4 Co-authorship Statement	10
1.4.1 Co-author Contributions-Chapter 2	10
1.4.2 Co-author Contributions-Chapter 3	10

2	Random Vibration Response of a Spur Gear Pair with Periodic Stiffness and Backlash	11
2.1	Introduction	11
2.2	Mechanical Model	12
2.3	Curve Fitting	15
2.4	Path Integration	16
2.5	Simulation Results	18
2.6	Conclusions	24
3	Random Dynamics of a Nonlinear Spur Gear Pair in Probabilistic Domain	25
3.1	Introduction	25
3.2	Mechanical Model	26
3.3	Path Integration	30
3.3.1	Short Time Transition PDF	31
3.3.2	Time and space discretization	33
3.4	Simulation	34
3.5	Conclusions	41
4	Random Response of a Single Stage Gear Rattling System	43
4.1	Introduction	43
4.2	Mechanical Model	44
4.3	Path Integration	46
4.4	Simulation	47
4.5	Conclusions	53
5	Conclusions and Future Work	54
5.1	Conclusions	54

5.2 Future Work	55
Bibliography and References	57
Appendices	62

List of Tables

2.1 Deterministic results of x and v 22

List of Figures

2.1	Mechanical model of the gear pair	12
2.2	Curve fitting of backlash nonlinearity function	16
2.3	Displacement in deterministic case	19
2.4	Velocity in deterministic case	19
2.5	Evolution of probability distribution.	20
2.6	Probability distribution.	21
2.7	Contour of probability distribution.	23
2.8	Contour of probability distribution at 25T with different r.	24
3.1	Model of the gear system	26
3.2	Gear mesh stiffness	27
3.3	Displacement response in deterministic case ($\Omega_m = 0.75$).	35
3.4	Velocity response in deterministic case ($\Omega_m = 0.75$).	35
3.5	Domains of attraction ($\Omega_m = 0.75$).	36
3.6	Joint distribution($\Omega_m = 0.85, r = 0.0009, t = 40T$). (a) Monte Carlo simulation; (b) path integration.	36
3.7	Marginal distribution ($\Omega_m = 0.85, r = 0.0009, t = 40T$). (a) displacement; (b) velocity.	37
3.8	Joint distribution($\Omega_m = 0.75, r = 0.0004, t = 30T$). (a) Monte Carlo simulation; (b) path integration.	38

3.9	Marginal distribution ($\Omega_m = 0.75$, $r = 0.0004$, $t = 30T$). (a) displacement; (b) velocity.	38
3.10	Surface plot of probability distribution. (a) $39\frac{1}{4}T$; (b) $39\frac{2}{4}T$; (c) $39\frac{3}{4}T$; (d) $40T$	39
3.11	Contour plot of probability distribution. (a) $39\frac{1}{4}T$; (b) $39\frac{2}{4}T$; (c) $39\frac{3}{4}T$; (d) $40T$	40
4.1	Model of rattling	44
4.2	Displacement response in deterministic case.	48
4.3	Velocity response in deterministic case.	48
4.4	Phase plot.	49
4.5	Joint distribution ($s = 0.9$, $t = 188.496$). (a) Monte Carlo simulation; (b) path integration.	50
4.6	Marginal distribution ($s = 0.9$, $t = 188.496$). (a) displacement; (b) velocity.	50
4.7	Surface plot of probability distribution ($s = 0.9$). (a) $t = 246.615$; (b) $t = 248.186$; (c) $t = 249.757$; (d) $t = 251.327$	51
4.8	Surface plot of probability distribution ($s = 0.8$). (a) $t = 246.615$; (b) $t = 248.186$; (c) $t = 249.757$; (d) $t = 251.327$	52
4.9	Joint probability distribution with different white noise intensities ($s = 0.9$, $t = 251.327$). (a) $r = 0.0025$; (b) $r = 0.0075$	53

Chapter 1

Introduction

1.1 Scope of the Research

The aim of the research is to apply the path integration method to the stochastic nonlinear model of a spur gear pair considering both backlash and time-varying mesh stiffness and investigate its random response, which includes:

- investigating the accuracy of the path integration method applied in different stochastic nonlinear gear models.
- investigating the probability distribution of displacement and velocity responses under both deterministic and random loads.
- investigating the complicated nonlinear phenomena in random case, such as multiple coexisting stable motions and chaotic motions.

Different stochastic nonlinear gear models are investigated in Chapters 2–4 depending on the approximation of backlash nonlinearity and time-varying mesh stiffness:

1. **Smoothing backlash nonlinearity and harmonic approximation of mesh stiffness** (Chapter 2). The backlash nonlinearity is simplified as a softening cubic nonlinearity by curve fitting and the time-varying mesh stiffness is represented as a constant plus a cosinusoidal component. In this case, only the single-sided impact is considered.
2. **Piecewise linear backlash nonlinearity and square wave approximation of mesh stiffness** (Chapter 3). The backlash nonlinearity is represented as a piecewise linear function and the time-varying mesh stiffness is approximated as a square wave function.
3. **Rattling model** (Chapter 4). This is a rigid vibro-impact model considering only backlash. The abrupt change of velocity occurs when impact happens.

1.2 Thesis Outline

Chapter 1 includes an introduction of the research scope and brief review of previous research on gear dynamics from the mathematical models, analytical and numerical algorithms aspects.

Chapter 2 investigates the random response of the gear model with smoothing backlash nonlinearity and harmonic approximation of mesh stiffness under single-sided impact. The Gaussian closure procedure is applied to obtain the mean and variance of transition PDF.

Chapter 3 investigates the random response of the gear model with piecewise linear backlash nonlinearity and square wave approximation of mesh stiffness. A new procedure to calculate the variance is presented. Multiple coexisting stable motions are

captured with certain parameter values.

Chapter 4 is the investigation of random response of a gear rattling model. A degenerate form of transition PDF is employed and aperiodic motion is observed in deterministic case.

Chapter 5 is the summary of various approaches of path integration methods applied to different gear models in Chapters 2–4. Meanwhile, topics for further research are also discussed.

1.3 Literature Review

The application of gears could be found from drilling in offshore platforms to spacecrafts in aerospace, from automobiles in daily life to machine tools in industry. The wide application of gears triggered intensive study on design, manufacture, dynamic performance, fatigue and reliability evaluation, etc., during the past decades. The study of dynamic performance could identify and estimate the elements which affect the working performance of gears and thus contribute to improving the gear design and manufacturing techniques. The following review focuses on the study of gear dynamics from modeling, methodology and dynamic response aspects.

1.3.1 Linear Gear Dynamics

Early studies of gear dynamics are based on a linear model. By assuming constant mesh stiffness, modeling equivalent mass and ignoring damping, a spring-mass model was proposed by Tuplin [1,2] to investigate the stress and load on gear teeth. Some

linear translational and torsional models with constant mesh stiffness were also summarized by Özgüven and Houser [3] in their review paper. The nonlinear factors, such as backlash between gear teeth and time-varying mesh stiffness due to the variation of contact area between gear teeth during the mesh cycle, could greatly affect the accuracy of dynamic load evaluation. Later models [4, 5] considered the time-varying mesh stiffness in the study of dynamic load. The linear model without considering these nonlinear factors could not capture the complicated nonlinear phenomena such as jump, multiple coexisting stable motions, subharmonic and superharmonic resonances and chaotic motions demonstrated in experiments by Kahraman and Blankenship [6]. Although the linear model could not reveal the nature of real gear dynamics, it laid the foundation for the later nonlinear gear model. More detailed linear gear models and approaches of solutions in deterministic gear dynamics could be found in literature [3].

1.3.2 Nonlinear Gear Dynamics

The multiple nonlinearities in gear systems such as backlash, time-varying mesh stiffness, static transmission error and friction between gear teeth [7] highlight the necessity of nonlinear gear modeling. The review by Wang, Li and Peng [7] classified the nonlinear model based on the nonlinear elements considered and the number of degree of freedom. They also reviewed various approaches to study the nonlinear dynamic response of gear systems including digital simulation [8–10], analog simulation [8], piecewise linear techniques [11], harmonic balance method (HBM) [8, 9, 12–14], perturbation method [15], model analysis method and shooting method. In addition to the methods summarized by Wang, Li and Peng [7], the direct numerical integration [12, 16], and finite element method [17] were also adopted in the study of deterministic nonlinear gear dynamics. The numerical results are relatively easier to

obtain than analytical results. And the numerical methods are frequently used to validate the analytical methods (see references [8, 9, 12, 16]).

As mentioned above, multiple nonlinearities exist in the real gear systems. The purpose of gear modeling is to simplify real gear systems properly without losing their dynamic nature. The nonlinear gear model in literature [6, 9, 10, 12–14, 16] considered only the two main nonlinearities in gear dynamics [7]—backlash and time-varying mesh stiffness. And the nonlinear gear model evolved from including only backlash [9] to including both backlash and time-varying mesh stiffness [10, 12–14, 16]. In the following part, literature is reviewed from nonlinear gear modeling, methodology and dynamic response aspects.

Kahraman and Singh [9] presented a nonlinear model of a spur gear pair considering only backlash. They summarized the excitation types from external and internal aspects, but the harmonic excitation in their model focused on the internal aspect. Digital simulation and HBM were adopted to get dynamic response of the gear system. Good agreement was found in the comparison between results from digital simulation and HBM, while some solutions were not captured by the numerical method, because the numerical solution greatly depends on the value of initial conditions in a multi-valued region. They also compared the analytical results with experimental results from Munro [18]. Although these two kinds of results were not well matched, the jump phenomenon in the frequency domain was well observed from both of them. They further conducted parametric studies by varying the value of excitation force to study the influence on dynamic response in the frequency domain. Nonlinear phenomena such as jump, multiple coexisting stable motions, superharmonic resonances and chaotic motions were observed from their plots.

Blankenship and Kahraman [12] presented a mechanical model considering both time-varying mesh stiffness and clearance which could be applied to describe the model of a spur gear pair. They adopted the HBM including multiple harmonics in the study of frequency response. Experiments were conducted by them to verify the HBM, and results from the HBM matched well with those from experiments. They also observed superharmonic resonance and multiple coexisting steady motions from experimental results. Parametric studies were conducted by varying the value of stiffness, damping ratio and preload to investigate their influence on response amplitude in the frequency domain. They extended their research (see reference [13]) on the study of subharmonic resonance from experimental and theoretical aspects. Parametric studies were also conducted by them to investigate the effect of phase angle and alternating force on response amplitude in the frequency domain.

Theodossiades and Natsisvas [16] presented a spur gear pair model considering both time-varying mesh stiffness and backlash. They proposed a new perturbation method which combined the piecewise linear techniques and classical perturbation. This method was applied to three cases: no impact, single-sided impact and double-sided impact. Results from direct integration was obtained to validate the accuracy and efficiency of the proposed method. Its validity was demonstrated by the good agreement between analytical results and numerical results. They also conducted parametric studies for the stiffness, damping, constant force, alternating force and phase angle. Chaotic motion was observed from their response history plot and Poincaré section.

1.3.3 Stochastic Gear Dynamics

The presence of random components in real gear systems is inevitable. They may come from internal aspects such as gear teeth profile deviation from manufacturing error and wear, or external aspects such as the torque fluctuation. Therefore, a gear model including random excitation is more realistic and necessary. Many nonlinear stochastic systems [19–23] modeled the random excitation as white noise with the advantage of easy mathematical treatment. The random response of such systems could be described as a Markov process and the PDF could be obtained by solving the Fokker-Planck equation [24]. Researchers [20, 21, 25] attempted to obtain numerical solutions of the Fokker-Planck equation by numerical methods such as path integration as the analytical solutions rarely exist in most cases [26].

Yu, Cai and Lin [25] proposed a new path integration method and applied it in several nonlinear stochastic systems excited by Gaussian white noise. By following the Gauss-Legendre scheme, the stationary probability densities obtained by path integration were compared with exact analytical solutions. Good agreement was observed between them.

Yu and Lin [20] investigated a non-homogeneous Markov process by path integration. The transition PDF was assumed as a Gaussian distribution. Moment equations were applied to obtain its mean and variance. They studied the jump phenomenon in the frequency domain and the existence of two stable motions in deterministic and random cases.

The development of a stochastic gear model provides a new perspective to investigate gear dynamics. The developed stochastic gear model could vary depending on

the nonlinear factors considered. Pfeiffer and Kunert [27] presented a stochastic gear model considering backlash in the study of the gear rattling problem. Wang and Zhang [28] presented a gear model randomly excited by transmission error. The time-varying mesh stiffness was also considered in their model. Naess, Kolnes and Mo [23] developed a stochastic gear model by adding white noise excitation. The backlash was considered in their model. However, the time-varying mesh stiffness which could lead to parametric vibration was not considered. Subsequently, Yang and Yang [29] presented a stochastic model considering both backlash and time-varying mesh stiffness in the study of random response of a spur gear pair. Yang [30] presented a two-stage stochastic gear model excited by deterministic force and white noise. In the following part, literature is reviewed from stochastic gear modeling, methodology and dynamic response aspects.

Pfeiffer and Kunert [27] developed mathematical models from deterministic to stochastic approach on a single stage gear rattling problem. The system governed by the Fokker-Planck equation was solved by finite difference method. They studied the Poincaré map along with the velocity probability distribution. The velocity probability distribution obtained from the Fokker-Planck equation was also compared with that from the point mapping equation. They further extended their study to the stochastic rattling model in gear-boxes in literature [31] with similar approach.

Naess, Kolnes and Mo [23] investigated a stochastic spur gear pair by path integration. In their approach, a degenerate Gaussian distribution was employed as a transition PDF whose variance is linearly changed with time step size. The mean of the transition PDF was obtained by a Runge-Kutta scheme and Newton iteration. They studied the influence of different forms of initial conditions and different parameter

values on the probability distribution. As the pioneering study on stochastic gear dynamics by path integration method, their gear model considered only backlash and the time-varying mesh stiffness was simplified as a constant. Afterwards, Mo and Naess [32] investigated the chaotic motion of a similar system by path integration. They presented the Poincaré map in deterministic case and joint probability distribution in random case.

Yang and Yang [29] investigated the random response of a spur gear pair by path integration. In their stochastic model, the time-varying mesh stiffness and backlash were both considered. With the application of numerical direct integration and statistic linearization technique, the mean and variance of transition PDF were obtained. They also studied the single-sided and double-sided impact in gear systems for both deterministic and random cases by varying the value of excitation force.

1.3.4 Summary of previous work

The mathematical model of gear systems has evolved from linear model to nonlinear model and stochastic nonlinear model. The linear model is no longer suitable to study the complex gear dynamics. The study within nonlinear scope has been intensive and complicated dynamic phenomena have been revealed. A more realistic stochastic model has been proposed by some researchers [23, 27–30, 32]. The current research of stochastic gear dynamics focuses on the application of numerical methods, and the complicated nonlinear phenomena such as multiple coexisting stable motions in random case are still under exploration.

1.4 Co-authorship Statement

The main purpose of this section is to illustrate the co-author contributions to the conference and journal papers presented in Chapter 2 and Chapter 3, respectively. In accordance with the thesis content and format, some content in the original papers is slightly changed and literature review is not presented in the thesis. The unmentioned work like programing and simulation was conducted by the thesis author.

1.4.1 Co-author Contributions-Chapter 2

Chapter 2 presents "Random Vibration Response of a Spur Gear Pair with Periodic Stiffness and Backlash", a conference paper accepted by American Society of Mechanical Engineers (ASME, IMECE2013). The modeling, smoothing of the backlash nonlinearity and approach to study random response of a spur gear pair were discussed by all authors. Among them, Dr. Jianming Yang contributed significantly to the smoothing of backlash nonlinearity. The simulation results were discussed between Dr. Jianming Yang and the thesis author. The draft was mainly written by the thesis author and revised by Dr. Jianming Yang.

1.4.2 Co-author Contributions-Chapter 3

Chapter 3 presents "Random Dynamics of a Nonlinear Spur Gear Pair in Probabilistic Domain", a journal paper accepted by Journal of Sound and Vibration. The proper modeling and adopted path integration method were the effort from all authors. Dr. Yang contributed significantly to the proposition of new procedure to calculate the variance of transition PDF. The simulation results were analyzed by Dr. Yang and the thesis author. The manuscript was written by Dr. Yang and the thesis author and the revision was conducted by Dr. Yang.

Chapter 2

Random Vibration Response of a Spur Gear Pair with Periodic Stiffness and Backlash

2.1 Introduction

This chapter investigates the random response of a spur gear pair under single-sided impact case. The spur gear pair under a combination of harmonic force and white noise excitation is modeled with the consideration of backlash and time-varying mesh stiffness. Path integration, as an effective numerical method to study the Markov Process, is applied to obtain the probability distribution. The backlash nonlinearity is treated with a cubic polynomial by curve fitting, which could contribute to the application of Gaussian closure procedure to obtain the mean and variance of transition PDF.

2.2 Mechanical Model

Figure 2.1 shows a pair of gears in mesh subjected to torque $T_1(t)$ and $T_2(t)$. The mesh stiffness changes periodically with time. This gear pair is governed by [29]:

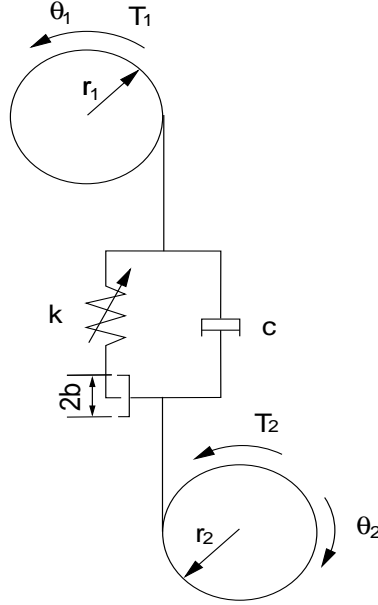


Figure 2.1: Mechanical model of the gear pair

$$J_1\ddot{\theta}_1 = T_1(t) - fr_1 \quad (2.1)$$

$$J_2\ddot{\theta}_2 = -T_2(t) + fr_2 \quad (2.2)$$

where J represents the moment of inertia, θ is the angular displacement, and r designates the radius of the base circle. The subscripts 1 and 2 represent gears 1 and 2, respectively. The meshing force f could be computed from

$$f = k(t)g(x) + c(r_1\dot{\theta}_1 - r_2\dot{\theta}_2) \quad (2.3)$$

where $k(t)$ and c are the time-varying mesh stiffness and damping coefficient, x is the relative displacement between gear teeth, and $g(x)$ is the backlash nonlinearity function expressed in the form:

$$g(x) = \begin{cases} x - b & \text{if } x > b \\ 0 & \text{if } -b \leq x \leq b \\ x + b & \text{if } x < -b \end{cases} \quad (2.4)$$

where $2b$ is the total backlash. After some mathematic manipulations and merging the two equations into one, the general form of motion could be represented in the following form:

$$m\ddot{x} + c\dot{x} + k(t)g(x) = F \quad (2.5)$$

where m and F are equivalent mass and force respectively expressed as:

$$x = r_1\theta_1 - r_2\theta_2 \quad (2.6)$$

$$m = \frac{J_1J_2}{J_1r_2^2 + J_2r_1^2} \quad (2.7)$$

$$F = \frac{J_2T_1(t)r_1 + J_1T_2(t)r_2}{J_1r_2^2 + J_2r_1^2} \quad (2.8)$$

Introducing the following parameters [16]:

$$\tilde{x} = \frac{x}{b} \quad (2.9)$$

$$\omega_0 = \sqrt{\frac{k_0}{m}} \quad (2.10)$$

$$\tilde{t} = \omega_0 t \quad (2.11)$$

$$\zeta = \frac{c}{2\sqrt{mk_0}} \quad (2.12)$$

$$\kappa(\tilde{t}) = \frac{k(t)}{k_0} \quad (2.13)$$

$$f_0 = \frac{F}{b\omega_0^2 m} \quad (2.14)$$

where k_0 is the average mesh stiffness in a mesh cycle. For simplicity, \tilde{x} and \tilde{t} are replaced with x and t respectively in the rest part of the chapter. Considering the excitation from static transmission error (internal excitation), a periodic excitation $f_1 \cos(\omega t)$ is added. In both external and internal excitations, there may be some random components which are represented by Gaussian white noise $W(t)$ with unit intensity in this chapter. Equation (2.5) can be rewritten as the following nondimensionalized form:

$$\ddot{x} + 2\zeta\dot{x} + \kappa(t)g(x) = f_0 + f_1 \cos(\omega t) + rW(t) \quad (2.15)$$

where ω is the ratio of mesh frequency to ω_0 , $\kappa(t)$ is approximated as a periodic function with the following form:

$$\kappa(t) = 1 + \varepsilon \cos(\omega t) \quad (2.16)$$

where ε is a small parameter. $g(x)$ is in the following form:

$$g(x) = \begin{cases} x - 1 & \text{if } x > 1 \\ 0 & \text{if } -1 \leq x \leq 1 \\ x + 1 & \text{if } x < -1 \end{cases} \quad (2.17)$$

2.3 Curve Fitting

The backlash nonlinearity in this chapter is approximated by a cubic function in the form below:

$$g(x) = a_0 + a_1x + a_3x^3 \quad (2.18)$$

This equation could be obtained through curve fitting by predefining the range of response. Given the fact that most gears are designed for power transmission, double-sided impact rarely happens. In addition, the equilibrium point moves to the right because of the static average load f_0 . This is to say that only a small portion of the motion will be in the backlash region. The range of response can be estimated by firstly solving the Eq. (2.15) without Gaussian white noise. This practice is justified by the fact that random noise is generally small compared with the deterministic loads. Considering both the range of response and the accuracy of curve fitting, the equilibrium point is located at the region where gear teeth are in contact. The function $g(x)$ is changed to

$$g(x) = \begin{cases} 0 & \text{if } -1.7 \leq x \leq -0.9 \\ x + 0.9 & \text{if } x > -0.9 \end{cases} \quad (2.19)$$

The curve fitting is implemented in Matlab; 261 evenly distributed points within the range $[-1.7 \ 0.9]$ are used. The results of the curve fitting are listed below:

$$a_0 = 0.9076, \quad a_1 = 1.096, \quad a_3 = -0.2035$$

The comparison between the cubic approximation and the original backlash nonlinearity function is shown in Fig. 2.2.

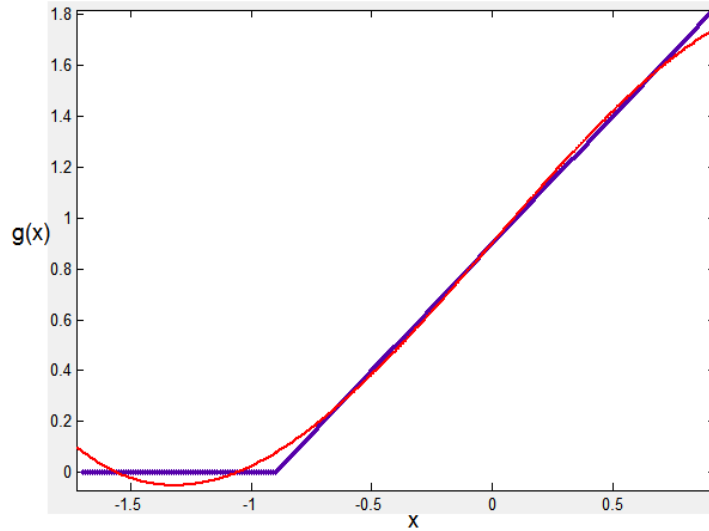


Figure 2.2: Curve fitting of backlash nonlinearity function

2.4 Path Integration

Path integration is a stepwise algorithm to calculate the probability density evolution. The probability density at n step $p(\mathbf{X}_n, t_n)$ is the integration of the product of probability density at previous step $p(\mathbf{X}_{n-1}, t_{n-1})$ and transition probability density $q(\mathbf{X}_n, t_n | \mathbf{X}_{n-1}, t_{n-1})$.

$$p(\mathbf{X}_n, t_n) = \int_R q(\mathbf{X}_n, t_n | \mathbf{X}_{n-1}, t_{n-1}) p(\mathbf{X}_{n-1}, t_{n-1}) d\mathbf{X}_{n-1} \quad (2.20)$$

With a given initial PDF and transition PDF, the probability density at n step can be obtained by this stepwise algorithm from the initial step as follows:

$$\begin{aligned}
p(\mathbf{X}_n, t_n) &= \int_R q(\mathbf{X}_n, t_n | \mathbf{X}_{n-1}, t_{n-1}) d\mathbf{X}_{n-1} \\
&\quad \int_R q(\mathbf{X}_{n-1}, t_{n-1} | \mathbf{X}_{n-2}, t_{n-2}) d\mathbf{X}_{n-2} \\
&\quad \dots \int_R q(\mathbf{X}_2, t_2 | \mathbf{X}_1, t_1) d\mathbf{X}_1 \int_R q(\mathbf{X}_1, t_1 | \mathbf{X}_0, t_0) p(\mathbf{X}_0, t_0) d\mathbf{X}_0 \quad (2.21)
\end{aligned}$$

In order to capture the probability distribution evolution of random response of the gear pair, the initial PDF and transition PDF need to be known. The former can be assumed as either deterministic or random form with certain distribution. In this chapter, it takes a Gaussian form (see Eq. (2.22)). The latter is approximated as a two-dimensional Gaussian distribution in a time step [20] in the following form:

$$p(x_0, \dot{x}_0) = \frac{1}{2\pi\sigma_{x_0}\sigma_{\dot{x}_0}} \exp \left\{ -\frac{(x_0 - \mu_{x_0})^2}{2\sigma_{x_0}^2} - \frac{(\dot{x}_0 - \mu_{\dot{x}_0})^2}{2\sigma_{\dot{x}_0}^2} \right\} \quad (2.22)$$

$$\begin{aligned}
q(x, \dot{x}) &= \frac{1}{2\pi\sigma_x\sigma_{\dot{x}}\sqrt{1-\rho^2}} \exp \\
&\quad \left(-\frac{1}{2(1-\rho^2)} \left[\frac{(x - \mu_x)^2}{\sigma_x^2} + \frac{(\dot{x} - \mu_{\dot{x}})^2}{\sigma_{\dot{x}}^2} - \frac{2\rho(x - \mu_x)(\dot{x} - \mu_{\dot{x}})}{\sigma_x\sigma_{\dot{x}}} \right] \right) \quad (2.23)
\end{aligned}$$

where μ is the mean, σ^2 is the variance and ρ is the correlation coefficient. Those parameters could be obtained by moment equations which was also adopted by Sun and Hsu [22]. Submitting Eqs. (2.16) and (2.18) into Eq. (2.15), yield

$$\ddot{x} + 2\zeta\dot{x} + (1 + \varepsilon \cos(\omega t)) (a_1x + a_3x^3) = f'_0 + f'_1 \cos(\omega t) + rW(t) \quad (2.24)$$

with

$$f'_0 = f_0 - a_0 \quad (2.25)$$

$$f'_1 = f_1 - \varepsilon a_0 \quad (2.26)$$

Based on Gaussian closure, the moment equations used to calculate the mean and variance of transition PDF are expressed as [20]:

$$\dot{m}_{10} = m_{01} \quad (2.27)$$

$$\dot{m}_{01} = -2\zeta m_{01} - (1 + \varepsilon \cos(\omega t)) \quad (2.28)$$

$$\begin{aligned} & \left[a_1 m_{10} + a_3 \left(-2m_{10}^3 + 3m_{10}m_{20} \right) \right] + f'_0 + f'_1 \cos(\omega t) \\ \dot{m}_{11} = m_{02} - 2\zeta m_{11} - (1 + \varepsilon \cos(\omega t)) \quad (2.29) \end{aligned}$$

$$\begin{aligned} & \left[a_1 m_{20} + a_3 \left(-2m_{10}^4 + 3m_{20}^2 \right) \right] + m_{10} (f'_0 + f'_1 \cos(\omega t)) \\ \dot{m}_{20} = 2m_{11} \quad (2.30) \end{aligned}$$

$$\dot{m}_{02} = -4\zeta m_{02} - 2(1 + \varepsilon \cos(\omega t)) \quad (2.31)$$

$$\begin{aligned} & \left[a_1 m_{11} + a_3 \left(-2m_{10}^3 m_{01} + 3m_{20} m_{11} \right) \right] \\ & + 2m_{01} (f'_0 + f'_1 \cos(\omega t)) + r^2 \end{aligned}$$

where $m_{ij} = E[x^i \dot{x}^j]$, $E[\cdot]$ is the assemble average.

2.5 Simulation Results

The simulation is conducted with the following parameter values:

$$\zeta = 0.05, \varepsilon = 0.065, \omega = 1.1, f_0 = 0.15, f_1 = 0.1, r = 0.06$$

For the initial PDF, the following parameter values are used.

$$\mu_{x_0} = -0.9, \mu_{\dot{x}_0} = 0, \sigma_{x_0}^2 = 0.02, \sigma_{\dot{x}_0}^2 = 0.02$$

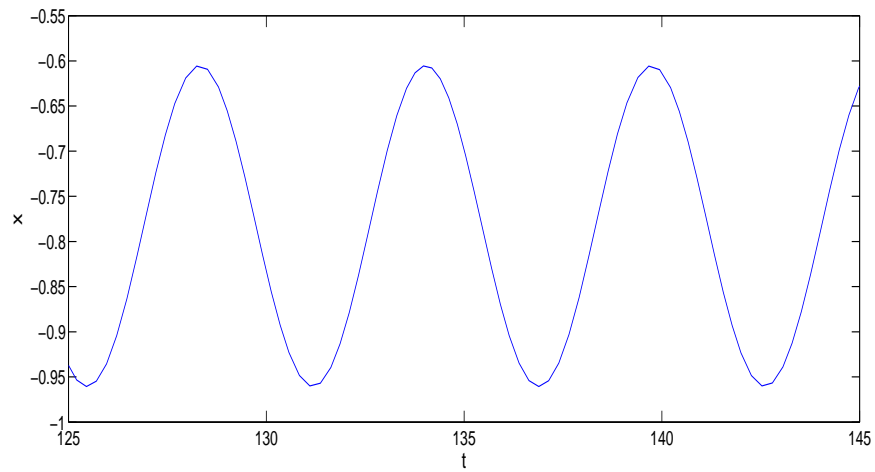


Figure 2.3: Displacement in deterministic case

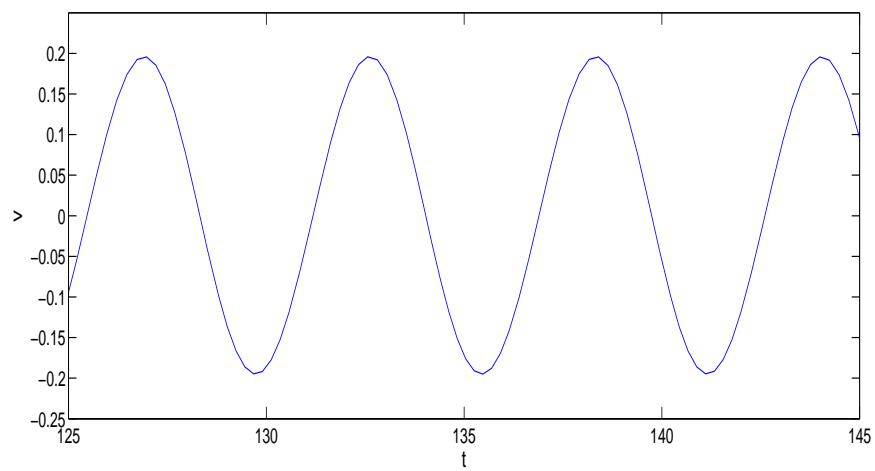


Figure 2.4: Velocity in deterministic case

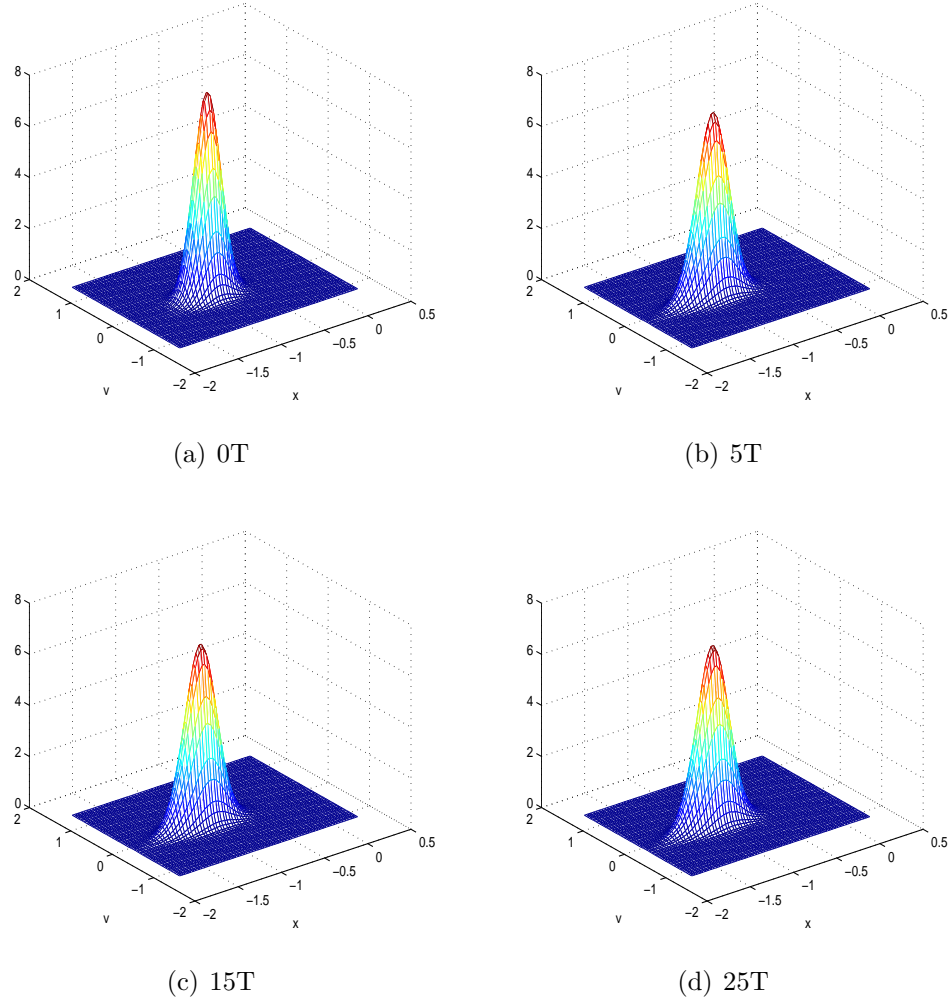


Figure 2.5: Evolution of probability distribution.

Before conducting the path integration, solution to the deterministic equation (Eq. (2.24) without the Gaussian white noise) is obtained through numerical integration. The results are shown in Fig. 2.3 and 2.4. The range of displacement is $[-0.96, -0.6]$, which corresponds to the single-sided impact. The velocity ranges from -0.2 to 0.2 . The moment equations are solved by 4th and 5th order adaptive step size Runge-Kutta method. The time step size is taken as $T/4$. And the state space is taken as $[-1.8, 0.29] \times [-1.2, 1.4]$ with 32×35 evenly distributed subintervals. With four

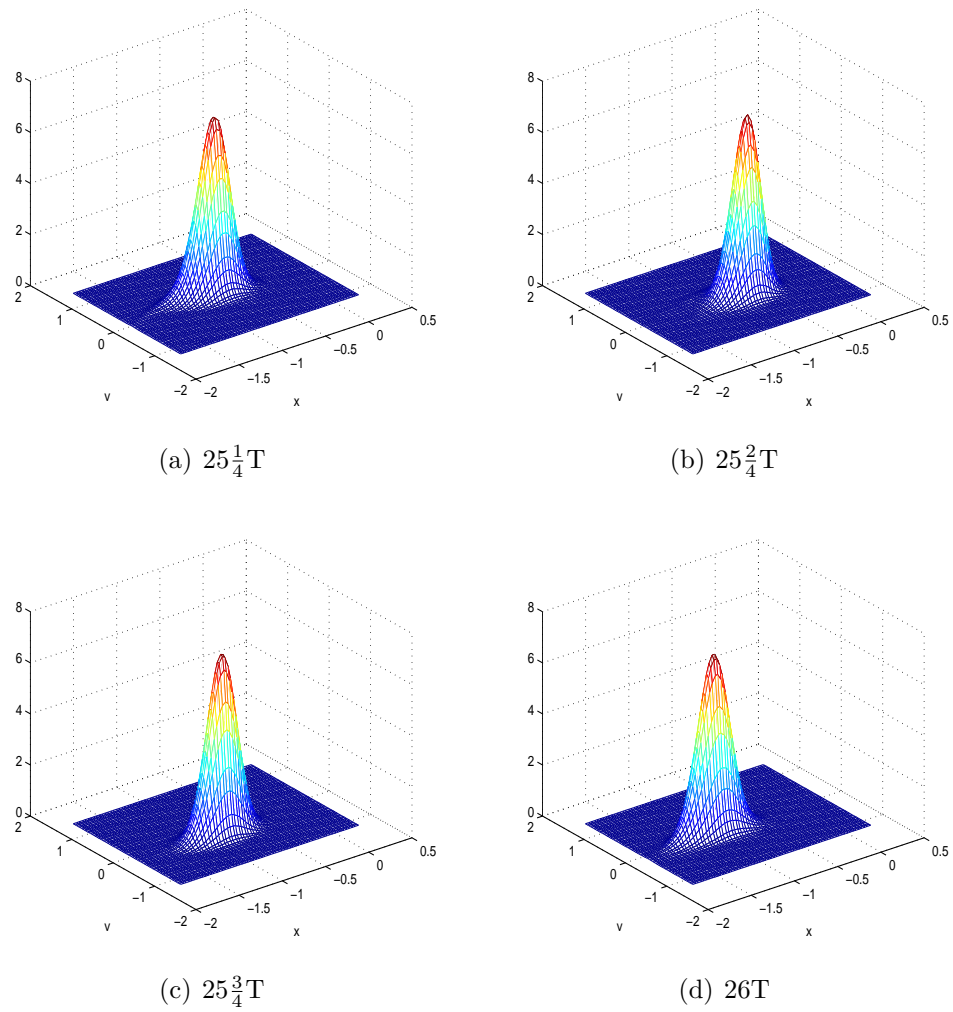


Figure 2.6: Probability distribution.

Gauss quadrature points in each subinterval, there are 64×70 points in total.

Figure 2.5 is the probability distribution at 0 , $5T$, $15T$ and $25T$. As can be seen, the probability distribution at $15T$ and $25T$ are almost the same, which indicates the response is stable after $15T$.

Figure 2.6 shows the probability distribution evolution within $25T$ from four sub-plots.

Table 1 records the deterministic results of displacement and velocity at corresponding time spots. For comparison purposes, those deterministic results are marked with "+" in the plane of (x,v) as shown in Fig. 2.7. Figure 2.7 is the contour plot of probability distribution corresponding to Fig. 2.6. As can be seen, the "+" marks are very close to the peak value of probability distribution, which means the probability distribution of random response is distributed around the deterministic results and the deviation between random response and deterministic results comes from the perturbation of Gaussian white noise. This good agreement between random response and deterministic results indicates the capability of path integration method in analysis of random response of the gear pair.

Figure 2.8 shows the contour of the probability distribution at $25T$, but with different intensities of Gaussian white noise. As can be seen, the probability distribution tends to spread out wider with stronger Gaussian white noise. This is straightforward and easy to understand.

Table 2.1: Deterministic results of x and v

Time	x	v
$25\frac{1}{4}T$	-0.7458	0.1921
$25\frac{2}{4}T$	-0.6098	-0.0436
$25\frac{3}{4}T$	-0.8230	-0.1896
$26T$	-0.9565	0.0411

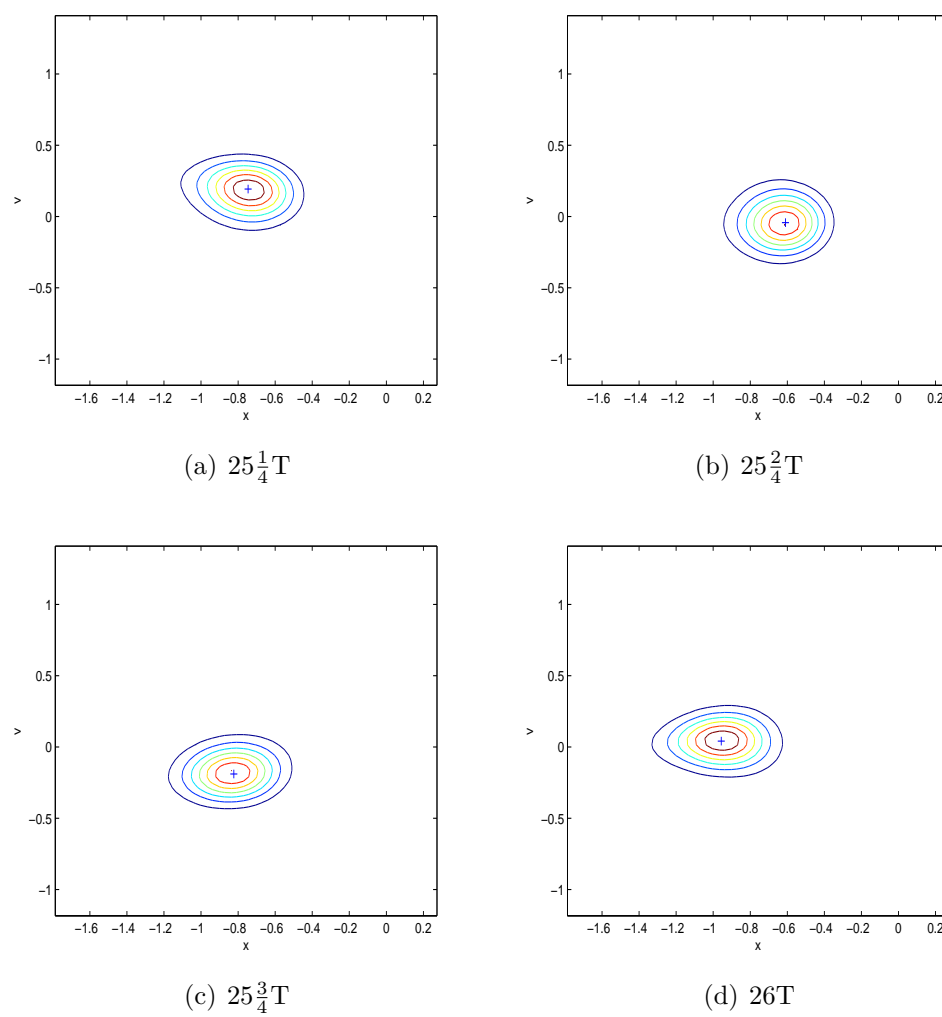


Figure 2.7: Contour of probability distribution.

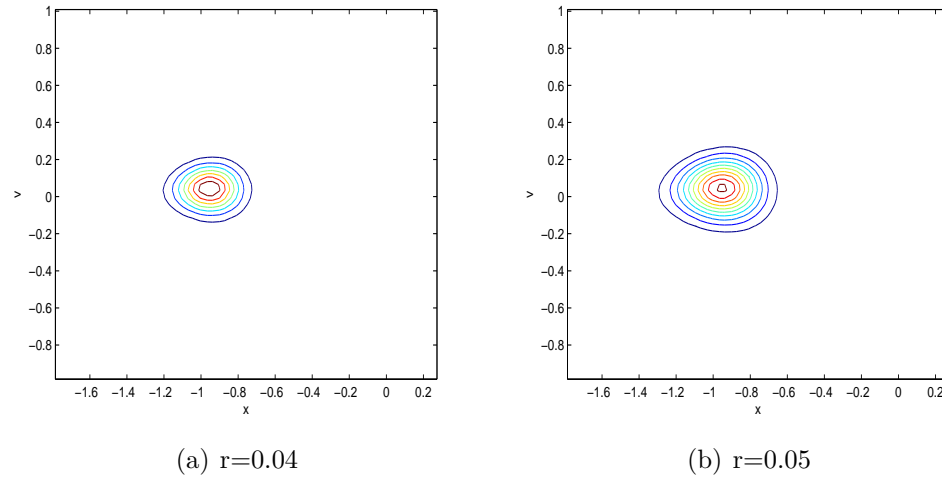


Figure 2.8: Contour of probability distribution at 25T with different r .

2.6 Conclusions

This chapter investigates the random vibration response of a spur gear pair with path integration method. Both time-varying mesh stiffness and backlash nonlinearity are accounted for in this model. The mesh stiffness is modeled as a constant plus a cosinusoidal component, and the discontinuous backlash nonlinearity is approximated with a cubic polynomial through curve fitting. In the curve fitting process, only the single-sided impact case is considered based on the fact that most gear pairs are for power transmission; therefore, double-sided impact rarely happens. The random results are compared with deterministic results. Good agreement is found between them, which shows the promising potential for path integration applied in random gear dynamics.

Chapter 3

Random Dynamics of a Nonlinear Spur Gear Pair in Probabilistic Domain

3.1 Introduction

This chapter investigates the random response of a spur gear pair including time-varying mesh stiffness and backlash by path integration method. In Chapter 2, the backlash nonlinearity is treated as a cubic polynomial, while it is directly represented as its original piecewise-linear form in this chapter. Gaussian closure procedure is thus inapplicable to obtain the mean and variance of the transition PDF due to the discontinuity of backlash nonlinearity. And the time-varying mesh stiffness is approximated as a square wave function in this chapter instead of a cosine function in Chapter 2. A new method to construct the transition PDF is presented and path integration results are validated by Monte Carlo simulation. The responses in deterministic and random cases are presented and compared in the time domain.

3.2 Mechanical Model

The system investigated in this chapter is shown in Fig. 3.1. It consists of two gears in mesh. For simplicity, only the rotation of the gears is considered. Without loss of generality, the vibration of the gears in rotation can be expressed as:

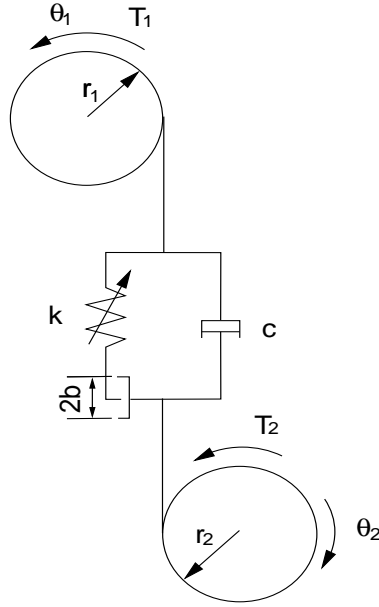


Figure 3.1: Model of the gear system

$$J_1 \ddot{\theta}_1 = T_1 - fr_1 \quad (3.1)$$

$$J_2 \ddot{\theta}_2 = -T_2 + fr_2 \quad (3.2)$$

where r_i, θ_i, T_i, J_i are the radius of the base circle, the rotational angular displacement, the input or output torque and the moment of inertia of gear i , respectively. Subscript i represents the number of the gear; in this case, $i = 1, 2$. The meshing force f between

the two gears is calculated by

$$f = kg(x) + c(r_1\dot{\theta}_1 - r_2\dot{\theta}_2) \quad (3.3)$$

where k and c are the mesh stiffness and the damping coefficient, respectively. $g(x)$ takes one of the three forms below depending on the value of displacement x .

$$g(x) = \begin{cases} x - b & \text{if } x \geq b, \\ 0 & \text{if } -b < x < b, \\ x + b & \text{if } x \leq -b. \end{cases} \quad (3.4)$$

$2b$ represents the total backlash. x is the relative linear displacement between the two meshing gears along the action line. The change of teeth number in contact during operation leads to the variation of gear mesh stiffness. Wang and Howard [33], Kiekbusch et al. [34] investigated the variation of mesh stiffness of spur gears using finite element methods. According to their research, the gear mesh stiffness could be approximated as a square wave as shown in Fig. 3.2.

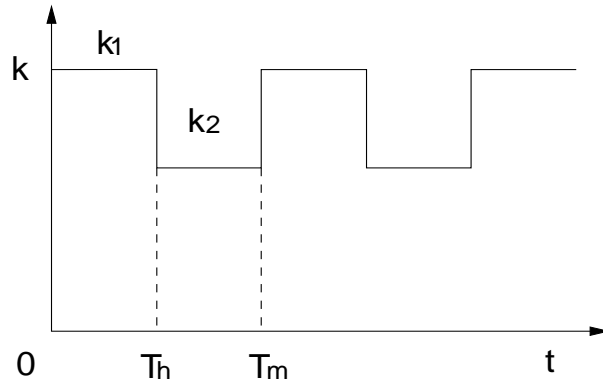


Figure 3.2: Gear mesh stiffness

$$k = \begin{cases} k_1 & \text{if } (n-1)T_m \leq t < (n-1)T_m + T_h, \\ k_2 & \text{if } (n-1)T_m + T_h \leq t < nT_m. \quad n = 1, 2, 3, \dots \end{cases} \quad (3.5)$$

where k_1 and k_2 are two different stiffness values. T_m is the mesh period of gear teeth. T_h represents the portion of time within a period corresponding to k_1 . Multiplying Eq. (3.1) by r_1/J_1 and Eq. (3.2) by r_2/J_2 , then subtracting the second from the first one gives the following equation after some manipulations:

$$\ddot{x} + \bar{c}\dot{x} + \bar{k}g(x) = F \quad (3.6)$$

The variables and parameters in the above equation are as follows:

$$x = r_1\theta_1 - r_2\theta_2 \quad (3.7)$$

$$\bar{c} = c(r_1^2/J_1 + r_2^2/J_2) \quad (3.8)$$

$$\bar{k} = k(r_1^2/J_1 + r_2^2/J_2) \quad (3.9)$$

$$F = T_1r_1/J_1 + T_2r_2/J_2 \quad (3.10)$$

Through the above transformation, the equation is simplified into a single degree-of-freedom system with time-varying stiffness and backlash nonlinearity.

Defining the following parameters [16]:

$$k_m = \left(\frac{T_h}{T_m} k_1 + \frac{T_m - T_h}{T_m} k_2 \right) (r_1^2/J_1 + r_2^2/J_2) \quad (3.11)$$

$$\omega_m = \sqrt{k_m} \quad (3.12)$$

$$\bar{t} = \omega_m t \quad (3.13)$$

$$\kappa = \frac{\bar{k}}{k_m} \quad (3.14)$$

$$u = \frac{x}{b} \quad (3.15)$$

$$\alpha = \frac{\bar{c}}{\sqrt{k_m}} \quad (3.16)$$

where t is time, k_m is the equivalent average mesh stiffness within one mesh cycle.

Eq. (3.6) can be changed to dimensionless form as below by applying the transformation from Eq. (3.11) to (3.16). And the excitation F is split into a constant deterministic part f_0 , a deterministic periodically changing part $f_1 \cos(\Omega_m \bar{t})$ and a random part $\xi(\bar{t})$.

$$\ddot{u} + \alpha \dot{u} + \kappa g(u) = f_0 + f_1 \cos(\Omega_m \bar{t}) + \xi(\bar{t}) \quad (3.17)$$

In the above equation, κ is a periodic function of dimensionless time \bar{t} . It takes the form as shown in Fig. 3.2. Ω_m is the ratio of mesh frequency to ω_m . \dot{u} and \ddot{u} are the first- and second-order derivatives with regard to dimensionless time \bar{t} , respectively. $g(u)$ takes one of the following three values:

$$g(u) = \begin{cases} u - 1 & \text{if } u \geq 1, \\ 0 & \text{if } -1 < u < 1, \\ u + 1 & \text{if } u \leq -1. \end{cases} \quad (3.18)$$

And $\xi(\bar{t})$ is Gaussian white noise with

$$E(\xi(\bar{t})) = 0 \quad (3.19)$$

$$E(\xi(\bar{t})\xi(\bar{t} + \tau)) = r\delta(\tau) \quad (3.20)$$

Eq. (3.17) is a parametric nonlinear equation. The \bar{t} is replaced by t for brevity in the remainder of the chapter. Numerous researchers [7, 16] have investigated such a system under only deterministic excitation. It can be rewritten as the following form with the transformation $u_1 = u$ and $u_2 = du_1/dt$:

$$\frac{du_1}{dt} = u_2 \quad (3.21)$$

$$\frac{du_2}{dt} = f_0 + f_1 \cos(\Omega_m t) - \alpha u_2 - \kappa g(u_1) + \xi(t) \quad (3.22)$$

The above equations can be further arranged into the so-called Ito's form and expressed in a compact matrix format as below.

$$d\mathbf{U}(t) = \mathbf{A}[\mathbf{U}, t]dt + \mathbf{B}[\mathbf{U}, t]d\mathbf{W}(t) \quad (3.23)$$

where $\mathbf{A}[\mathbf{U}, t]$ is the drift vector and $\mathbf{B}[\mathbf{U}, t]$ is the diffusion matrix, $d\mathbf{W}(t)$ is a standard Wiener vector process.

3.3 Path Integration

Path integration is a numerical procedure which describes the evolution of the PDF of a Markov process in time from an initial condition. It provides an alternative to directly numerical solution of the Fokker-Planck equation. The central idea of path integration is the assumption that a Markov process locally looks like a Gaussian

diffusion process. Therefore, the transition PDF can be expressed in closed form. In the following sections, the basic steps for carrying out path integration scheme are presented.

3.3.1 Short Time Transition PDF

Due to the periodic change of the mesh stiffness, the response of the gear pair may be non-stationary even under a stationary random excitation. For such a system, an exact, analytic solution of Eq. (3.17) is rarely known. A practical and more feasible alternative is to seek an approximately numerical solution. Path integration is such a method which assumes the transition PDF is Gaussian within a short time interval [22]. Several expressions exist in the literature [20, 22, 23] for the short time Gaussian transition PDF. In the present chapter, the one used by Yu et al. [20] as below is adopted:

$$\begin{aligned} q_i &= p(\mathbf{U}_i, t_i | \mathbf{U}_{i-1}, t_{i-1}) \\ &= \frac{1}{2\pi\sigma_1\sigma_2\sqrt{1-\rho^2}} e^{\left[-\frac{z}{2(1-\rho^2)}\right]} \end{aligned} \quad (3.24)$$

$$z = \frac{(u_1 - \mu_1)^2}{\sigma_1^2} - \frac{2\rho(u_1 - \mu_1)(u_2 - \mu_2)}{\sigma_1\sigma_2} + \frac{(u_2 - \mu_2)^2}{\sigma_2^2} \quad (3.25)$$

In the above equations, μ_j and σ_j ($j = 1, 2$) are the mean and the standard deviation of u_j , respectively. ρ is the correlation between u_1 and u_2 . μ_1 and μ_2 can be obtained through 4th and 5th order Runge-Kutta numerical integration to deterministic parts of Eqs. (3.21, 3.22) in each time step. Depending on the value of u , σ_1^2 , σ_2^2 and covariance σ_{12} can be expressed in closed form as described below.

If $u \geq 1$ or $u \leq -1$, the system takes a closed form to normal mass-damping-spring system subjected to stationary delta-correlated excitation and the following equations

apply [35]:

$$\sigma_1^2 = \frac{G_0}{4\xi\omega_0^3} \left(1 - e^{-2\xi\omega_0\Delta t} \left[\frac{\omega_0^2}{\omega_d^2} + \frac{\xi\omega_0}{\omega_d} \sin 2\omega_d\Delta t - \frac{\xi^2\omega_0^2}{\omega_d^2} \cos 2\omega_d\Delta t \right] \right) \quad (3.26)$$

$$\sigma_2^2 = \frac{G_0}{4\xi\omega_0} \left(1 - e^{-2\xi\omega_0\Delta t} \left[\frac{\omega_0^2}{\omega_d^2} - \frac{\xi\omega_0}{\omega_d} \sin 2\omega_d\Delta t - \frac{\xi^2\omega_0^2}{\omega_d^2} \cos 2\omega_d\Delta t \right] \right) \quad (3.27)$$

$$\sigma_{12} = \frac{G_0}{2\omega_d^2} e^{-2\xi\omega_0\Delta t} \sin^2 \omega_d\Delta t \quad (3.28)$$

with

$$G_0 = 2\pi r \quad (3.29)$$

$$\zeta = \frac{\alpha}{2\sqrt{\kappa}} \quad (3.30)$$

$$\omega_0 = \sqrt{\kappa} \quad (3.31)$$

$$\omega_d = \omega_0\sqrt{1 - \zeta^2} \quad (3.32)$$

If $-1 < u < 1$, it is a zero stiffness system and the following equations apply:

$$\sigma_1^2 = \frac{G_0}{\alpha^2} \left[\Delta t - \frac{1}{\alpha} \left(\frac{3}{2} - 2e^{-\alpha\Delta t} + \frac{1}{2}e^{-2\alpha\Delta t} \right) \right] \quad (3.33)$$

$$\sigma_2^2 = \frac{G_0}{2\alpha} \left(1 - e^{-2\alpha\Delta t} \right) \quad (3.34)$$

$$\sigma_{12} = \frac{G_0}{\alpha^2} \left[\frac{1}{2} - e^{-\alpha\Delta t} + \frac{1}{2}e^{-2\alpha\Delta t} \right] \quad (3.35)$$

Once σ_1, σ_2 and σ_{12} are known, ρ is calculated as below for both cases.

$$\rho = \frac{\sigma_{12}}{\sigma_1\sigma_2} \quad (3.36)$$

The derivation of Eqs. (3.33) to (3.35) is presented in the Appendices.

It is possible for some points starting in one case but ending in another case within a

time step. In this case, Δt_1 which represents the transition time between two different cases is estimated. Then the means μ_1 and μ_2 can be calculated by breaking the Δt into two parts and integrating the deterministic equations in corresponding case. For the variances σ_1^2, σ_2^2 and covariance σ_{12} , an equivalent stiffness is firstly approximated as below, then they are calculated by Eqs. (3.26) to (3.28).

$$k_e = \frac{\Delta t_e}{\Delta t} k \quad (3.37)$$

where Δt_e is the time when gear teeth are in contact and Δt is a time step size. Depending on the starting case, Δt_e is equal to either Δt_1 or $\Delta t - \Delta t_1$. The initial PDF takes a two-dimensional Gaussian form expressed as:

$$p(u_0, \dot{u}_0) = \frac{1}{2\pi\sigma_{u_0}\sigma_{\dot{u}_0}} \exp \left\{ -\frac{(u_0 - \mu_{u_0})^2}{2\sigma_{u_0}^2} - \frac{(\dot{u}_0 - \mu_{\dot{u}_0})^2}{2\sigma_{\dot{u}_0}^2} \right\} \quad (3.38)$$

3.3.2 Time and space discretization

The time step size in the above process should be carefully considered. If it is too large, computation error would increase and the real transition PDF may significantly deviate from the normal assumption. While if it is too small, the computation time would be too long. In this chapter, it is taken as $T/12$.

The ranges of u_1 and u_2 need to be appropriately estimated beforehand as well. In this chapter they are estimated within $[-1.8 \ 3.2] \times [-1.8 \ 1.8]$ for displacement and velocity, respectively. The number of sub-areas discretized in this area could vary depend on the smoothness level and computation time of the results. In each of the sub-area, four Gaussian quadrature points are used to maintain accuracy.

3.4 Simulation

The parameters used in the simulation are listed below:

$$\alpha = 0.1, f_0 = 0.4, f_1 = 0.1$$

$$\kappa = \begin{cases} 1.2 & (n-1)T \leq t < (n-1)T + T/2, \\ 0.8 & (n-1)T + T/2 \leq t < nT. \quad n = 1, 2, 3, \dots \end{cases}$$

The parameters used in the initial PDF are as below:

$$\mu_{u_0} = 1.1, \mu_{\dot{u}_0} = 0, \sigma_{u_0}^2 = 0.04, \sigma_{\dot{u}_0}^2 = 0.04$$

Before conducting simulation in random case, the deterministic part of the responses are firstly sought by setting the random part as zero. u_1 and u_2 are replaced with x and v for brevity from Fig. 3.3 to 3.11. When Ω_m is set to be 0.75, two stable solutions exist. Figures 3.3 and 3.4 show the displacement and velocity obtained for the two stable solutions. It is well known that which solution the system takes depends on the initial conditions. To get a clear picture on the effect of the initial conditions, Fig. 3.5 illustrates the domains of attraction under different initial conditions.

In the simulation of the random case, Ω_m is firstly set to be 0.85 and the intensity of Gaussian white noise r is 0.0009. For comparison purposes, Monte Carlo simulation is conducted as well with the same parameters. Figures 3.6 and 3.7 show the joint and marginal probability distributions of u_1 and u_2 respectively at time $40T$. Some samples in Monte Carlo simulation results are distributed far away from the peak, which could result in the deviation of peak height between path integration and Monte Carlo simulation. But in general, good agreement could be found between them.

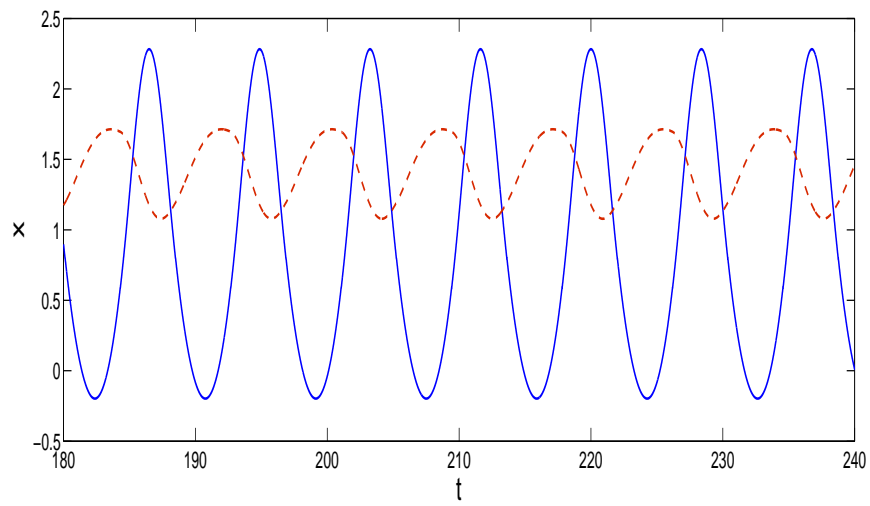


Figure 3.3: Displacement response in deterministic case ($\Omega_m = 0.75$).

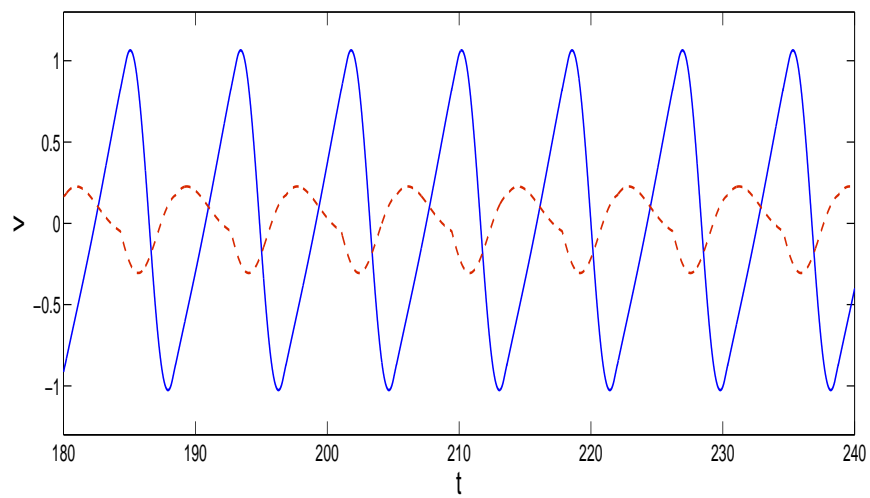


Figure 3.4: Velocity response in deterministic case ($\Omega_m = 0.75$).

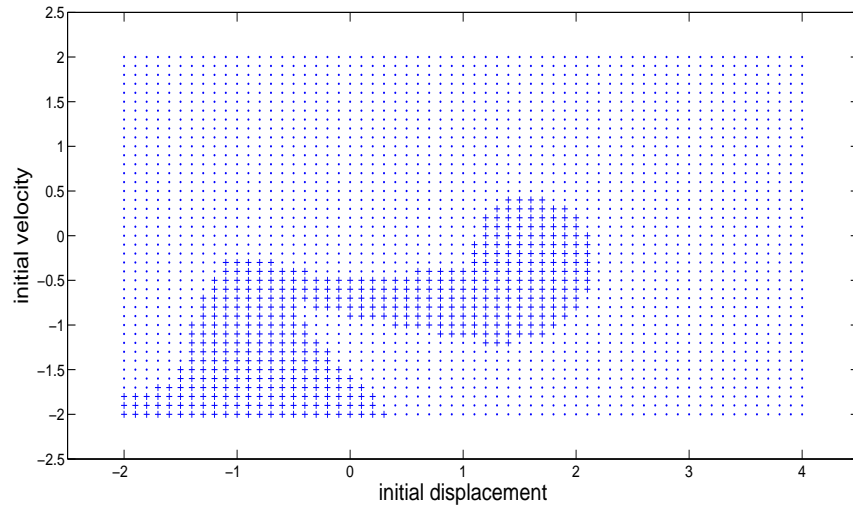


Figure 3.5: Domains of attraction ($\Omega_m = 0.75$).

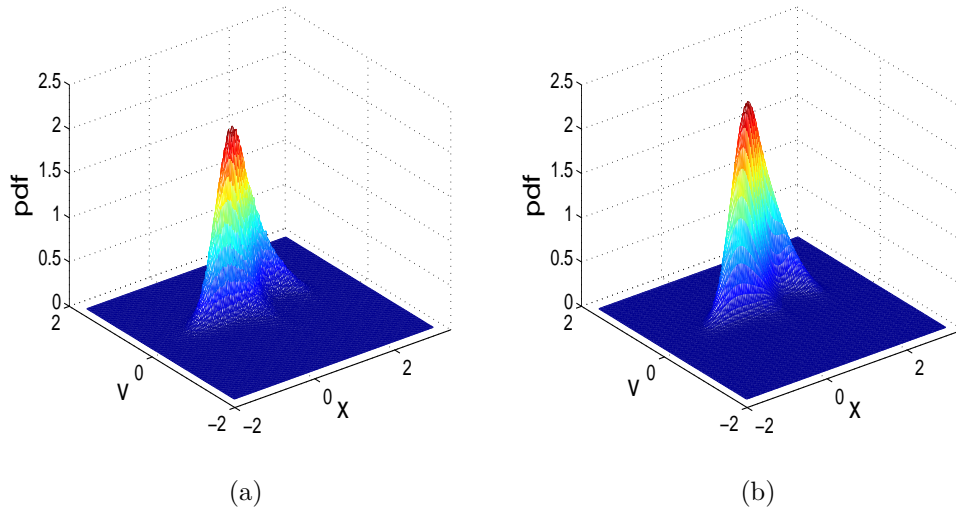


Figure 3.6: Joint distribution ($\Omega_m = 0.85$, $r = 0.0009$, $t = 40T$). (a) Monte Carlo simulation; (b) path integration.

It has been proven that multi-solutions exist for gear systems with backlash nonlinearity [16]. To capture this nonlinear feature, the simulation parameters are changed to

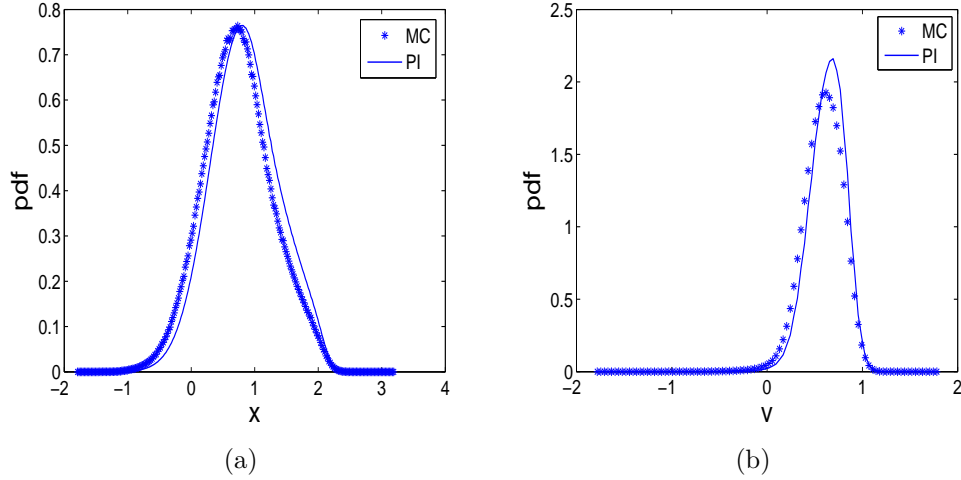


Figure 3.7: Marginal distribution ($\Omega_m = 0.85$, $r = 0.0009$, $t = 40T$). (a) displacement; (b) velocity.

be $\Omega_m=0.75$ and $r=0.0004$. Similar to the previous case, both path integration and Monte Carlo simulation are conducted with the same simulation parameters. The comparison between results from the two methods are illustrated in Figs. 3.8 and 3.9. Figure 3.8 shows the joint probability distributions of u_1 and u_2 , while Fig. 3.9 illustrates the marginal probability distributions of u_1 and u_2 at time $30T$.

It is observed that the results from path integration agree with that from Monte Carlo simulation, especially in the tail regions. However, the discrepancy in this multi-solutions case is bigger than that in the single solution case (Fig. 3.6 and 3.7), especially in the peak areas. This discrepancy could be caused by several reasons, such as numerical errors, discretization of time and space, sample size of Monte Carlo simulation, and initial conditions. The initial conditions of Monte Carlo simulation are points randomly distributed around the point $(1.1, 0)$ with Gaussian distribution. And the initial conditions of path integration are Gaussian quadrature points in grids distributed around the point $(1.1, 0)$. The initial conditions of Monte Carlo

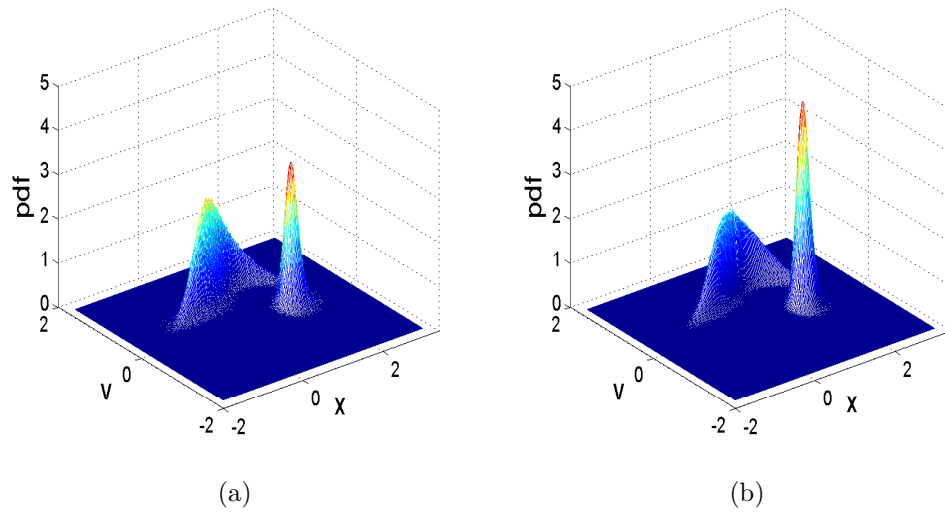


Figure 3.8: Joint distribution ($\Omega_m = 0.75$, $r = 0.0004$, $t = 30T$). (a) Monte Carlo simulation; (b) path integration.

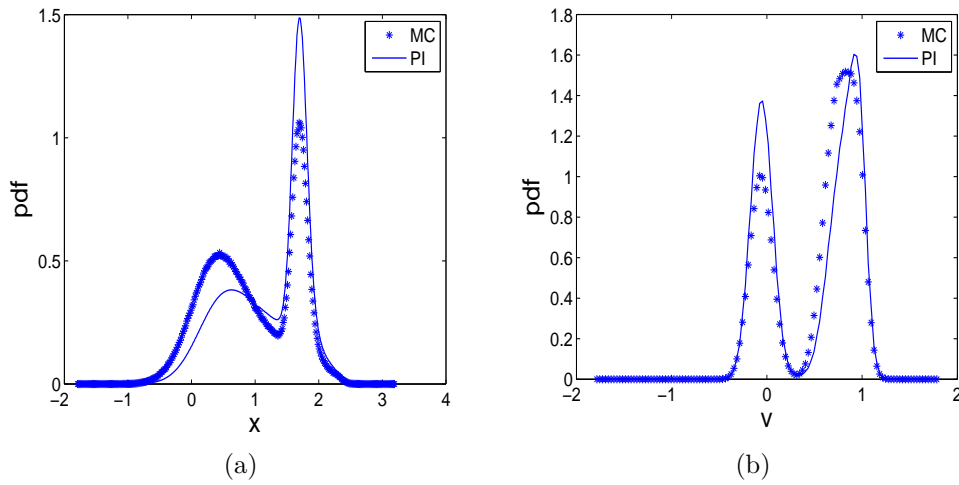


Figure 3.9: Marginal distribution ($\Omega_m = 0.75$, $r = 0.0004$, $t = 30T$). (a) displacement; (b) velocity.

simulation and path integration cover two different attraction areas in Fig. 3.5. In the multi-solutions case, when a small grid covers the boundary of different attraction domains in Fig. 3.5, the four Gaussian quadrature points in the grid used in the

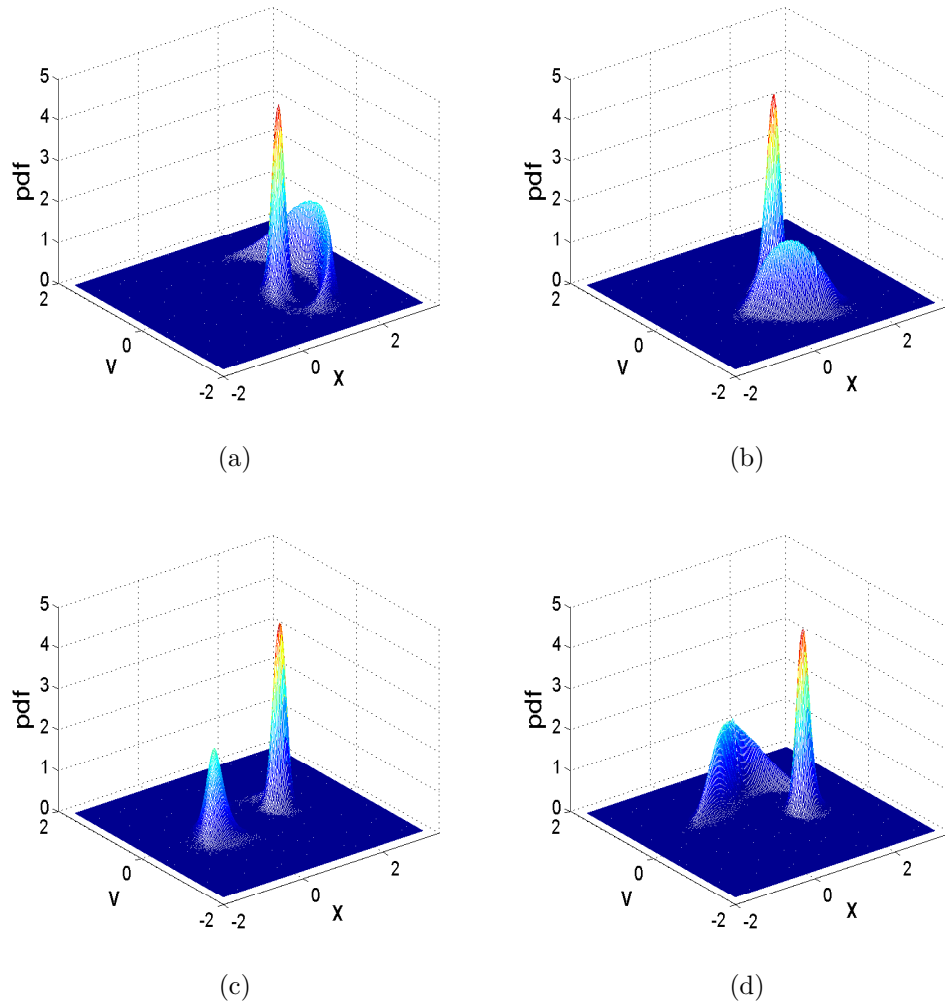


Figure 3.10: Surface plot of probability distribution. (a) $39\frac{1}{4}T$; (b) $39\frac{2}{4}T$; (c) $39\frac{3}{4}T$; (d) $40T$.

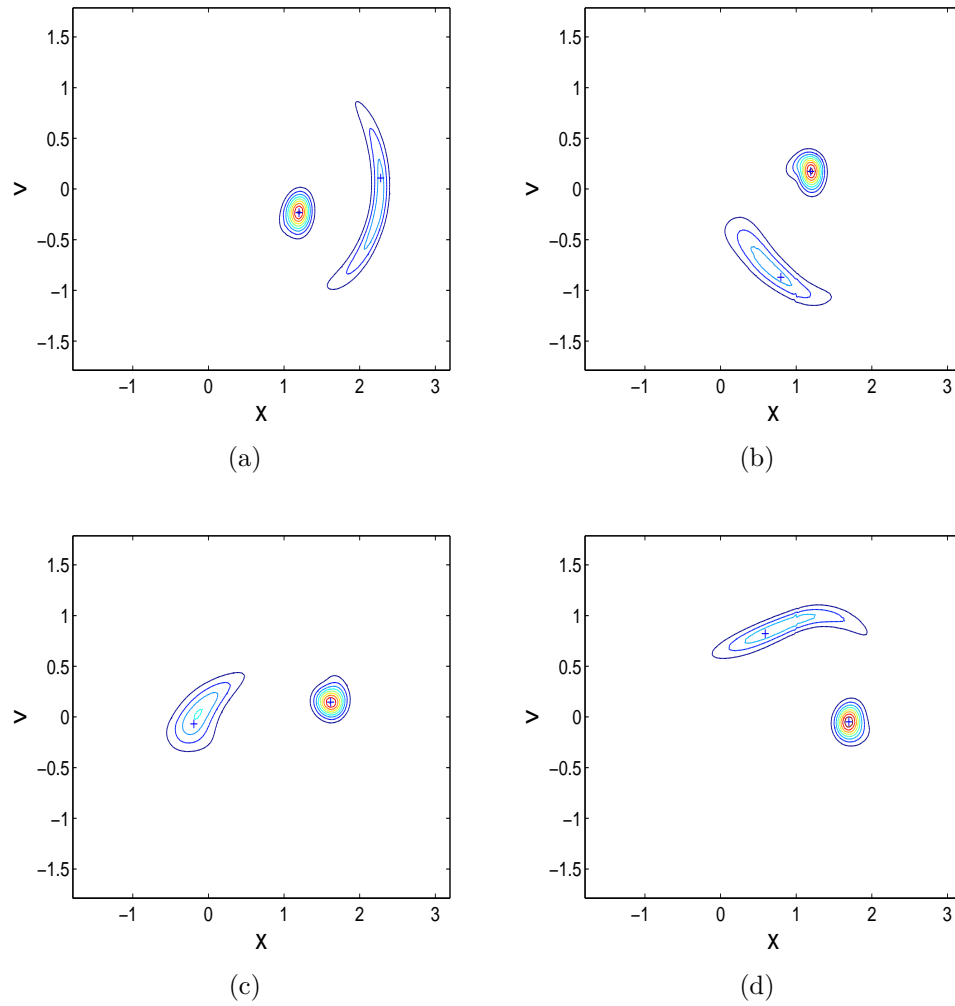


Figure 3.11: Contour plot of probability distribution. (a) $39\frac{1}{4}T$; (b) $39\frac{2}{4}T$; (c) $39\frac{3}{4}T$; (d) $40T$.

path integration could not represent the attraction tendency of the whole grid. This discrepancy will always exist as long as there are small areas covering the attraction boundary. However, this discrepancy could be controlled by making the grid areas covering the attraction boundary as small as possible through uneven partition of the solution range space. This has not been done yet in this chapter, and will be examined in future. However, this discrepancy does not hinder the significance of this method. As indicated by Naess and Johnsen [36,37], the real power of path integration lies in estimating the probability distribution of the tail regions which are particular interest in reliability study dealing with low probability events. It is obvious that the results of path integration and Monte Carlo simulation agree well in the tail regions in Fig. 3.9. The two obvious peaks in these figures indicate that two solutions exist in this system.

Figure 3.10 depicts the change of the probability distribution within one period. The four sub-plots show the probability distributions at four equally spaced time instants within the 39th period. The contour plot of Fig. 3.10 is given in Fig. 3.11. The corresponding solutions of the deterministic case at the same time instants are also shown in the sub-plots with the mark +. As expected, the solutions of the random case are around the deterministic ones. This is exactly the diffusion effect caused by the random excitation. This fact verifies that the path integration method in this chapter indeed captures the multi-solutions in the dynamic response of the nonlinear gear system.

3.5 Conclusions

This chapter investigates the random dynamics of a spur gear pair under harmonic and white noise excitation. Two important features in gear dynamics, time-varying mesh

stiffness and backlash nonlinearity, are accounted for in the model. The probability distribution evolution of the responses is examined with path integration method. The variance which constructs transition PDF is presented as different closed forms depending on the value of displacement. The results of path integration are compared with that of Monte Carlo simulation and deterministic results. Good agreements are found between them. The multi-solutions feature is also captured in the simulation results.

Chapter 4

Random Response of a Single Stage Gear Rattling System

4.1 Introduction

The existence of backlash in gear systems could lead to repeated impact. Two different models, rigid and elastic impacting body models [8], were widely employed in the study of gear dynamics [8,9,27,31]. The first model was commonly used to study the rattling problem in automobile transmission systems [27,31,38]. The second model was widely used to study more general gear systems [8–10,16,23]. Rattling could be commonly found in automobile transmission systems due to the lightly loaded or unloaded driven gear [27]. This chapter presents the application of path integration method in gear rattling problems. Unlike the elastic impacting body model employed in chapters 2 and 3, the rigid impacting body model is adopted in this chapter. The mathematical gear models could be simplified based on different applications. For instance, the influence of the backlash between gear teeth could be neglected in a heavily loaded gear system. For a rattling system, the influence from mesh

stiffness is neglected and a restitution coefficient is introduced when impact happens. The stochastic rattling model was firstly studied by Pfeiffer and Kunert [27, 31]. By solving the Fokker-Planck equation with finite differencing methods, they investigated the velocity distribution at one backlash boundary. The response of a rattling system under white noise excitation is a Markov process. The path integration method was widely used to investigate the random response of the Markov process (see references [20, 22, 25]). The system nonlinearity comes from the backlash between mesh gear teeth and abrupt velocity change when impact occurs. The deterministic and random responses in the time domain are investigated. Monte Carlo simulation is conducted as well to verify the accuracy of the applied path integration method.

4.2 Mechanical Model

The single stage rattling model investigated in this chapter is based on the model used by Pfeiffer and Kunert [27] as shown in Fig. 4.1.

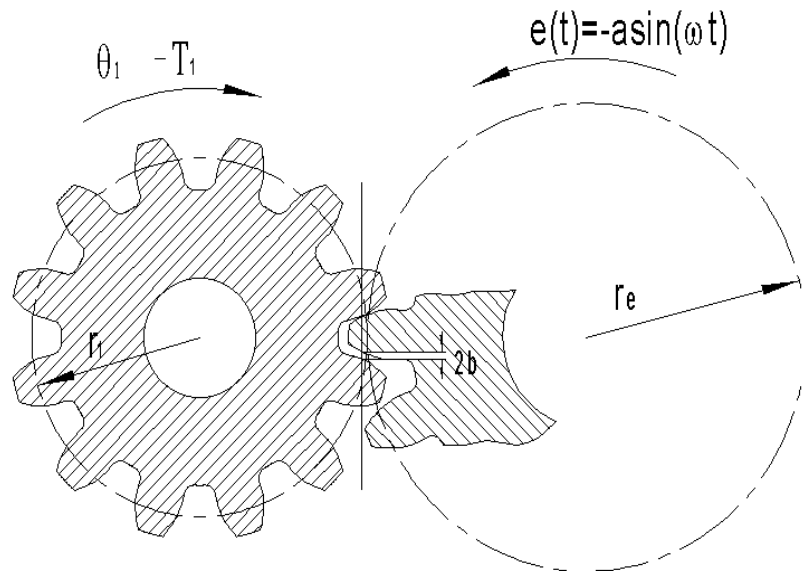


Figure 4.1: Model of rattling

When the gear teeth are under no contact, the system is governed by [27]:

$$I_1\ddot{\theta}_1 + d_1\dot{\theta}_1 = -T_1 \quad (4.1)$$

where I_1 represents the moment inertia, θ_1 , d_1 and T_1 are angular displacement, damping ratio and torque, respectively. When an impact occurs, the relative velocity between driven gear and driving gear changes both the amplitude and direction as:

$$v_r^+ = -sv_r^- \quad (4.2)$$

where v_r^+ , v_r^- are relative velocities immediately after and before an impact respectively, s is the restitution coefficient. As shown in Fig. 4.1, $2b$, r_1 , r_e and $e(t)$ are total backlash, radius of the base circle and harmonic rotation displacement with amplitude a and frequency ω , respectively. Defining the following parameters [27]:

$$\bar{t} = \omega t \quad (4.3)$$

$$x = \frac{e(t) - r_1\theta_1}{b} \quad (4.4)$$

$$\alpha = \frac{d_1}{I_1\omega} \quad (4.5)$$

$$f_0 = \frac{T_1 r_1}{I_1 b \omega^2} \quad (4.6)$$

$$f_1 = \frac{a}{b} \quad (4.7)$$

Considering the excitation from the random component, Eq. (4.1) could be transformed into a dimensionless form by applying the transformation from Eq. (4.3) to (4.7) in the free flight phase:

$$\ddot{x} + \alpha\dot{x} = f_0 + f_1(\sin(\bar{t}) - \alpha \cos(\bar{t})) + W(\bar{t}) \quad (4.8)$$

And $W(\bar{t})$ is Gaussian white noise with

$$E(W(\bar{t})) = 0 \quad (4.9)$$

$$E(W(\bar{t})W(\bar{t} + \tau)) = r\delta(\tau) \quad (4.10)$$

And for the impact moment ($x = \pm 1$),

$$\dot{x}^+ = -s\dot{x}^- \quad (4.11)$$

The \bar{t} is replaced by t for brevity in the remainder of the chapter. Two-dimensional stochastic differential equations could be obtained from Eq. (4.8) by defining $x_1 = x$ as follows:

$$\frac{dx_1}{dt} = x_2 \quad (4.12)$$

$$\frac{dx_2}{dt} = -\alpha x_2 + f_0 + f_1(\sin(t) - \alpha \cos(t)) + W(t) \quad (4.13)$$

4.3 Path Integration

The basic form of path integration could be expressed as:

$$p(\mathbf{X}_n, t_n) = \int_R q(\mathbf{X}_n, t_n | \mathbf{X}_{n-1}, t_{n-1}) p(\mathbf{X}_{n-1}, t_{n-1}) d\mathbf{X}_{n-1} \quad (4.14)$$

where $p(\mathbf{X}_n, t_n)$ and $q(\mathbf{X}_n, t_n | \mathbf{X}_{n-1}, t_{n-1})$ are probability density at n step and transition PDF from $n-1$ step to n step. Based on this stepwise algorithm, $p(\mathbf{X}_n, t_n)$ could be calculated with given initial PDF and transition PDF. As demonstrated by Sun and Hsu [22], the transition PDF could be assumed as Gaussian within a short time for the nonlinear system excited by Gaussian white noise. A degenerate multidimen-

sional Gaussian transition PDF used by Naess et al. [23] is employed in this chapter, which could be expressed as:

$$q(\mathbf{X}_n, t_n | \mathbf{X}_{n-1}, t_{n-1}) = \delta(x_1 - \mu_{x_1}) \frac{1}{\sqrt{2\pi r \Delta t}} \exp\left(-\frac{(x_2 - \mu_{x_2})^2}{2r \Delta t}\right) \quad (4.15)$$

where μ , $r\Delta t$ and $\delta(\cdot)$ are mean, variance and Dirac delta function, respectively. The mean could be obtained by 4th and 5th order Runge-Kutta numerical integration to deterministic parts of Eqs. (4.12, 4.13) in each time step. The initial PDF takes a two-dimensional Gaussian format expressed as below:

$$p(x_0, \dot{x}_0) = \frac{1}{2\pi\sigma_{x_0}\sigma_{\dot{x}_0}} \exp\left\{-\frac{(x_0 - \mu_{x_0})^2}{2\sigma_{x_0}^2} - \frac{(\dot{x}_0 - \mu_{\dot{x}_0})^2}{2\sigma_{\dot{x}_0}^2}\right\} \quad (4.16)$$

4.4 Simulation

The simulation is conducted with the following parameter values:

$$\alpha = 0.05, \quad f_0 = 0.1, \quad f_1 = 0.3, \quad r = 0.005$$

And for initial PDF, the following parameter values are used:

$$\mu_{x_0} = 0, \quad \mu_{\dot{x}_0} = 0.5, \quad \sigma_{x_0}^2 = 0.01, \quad \sigma_{\dot{x}_0}^2 = 0.01$$

Contrary to random response, the displacement and velocity responses are investigated in deterministic case as shown in Figs. 4.2 and 4.3. No periodic solution could be found from them. This aperiodicity could be further demonstrated by the phase plot in Fig. 4.4. As can be seen, stable motion does not exist.

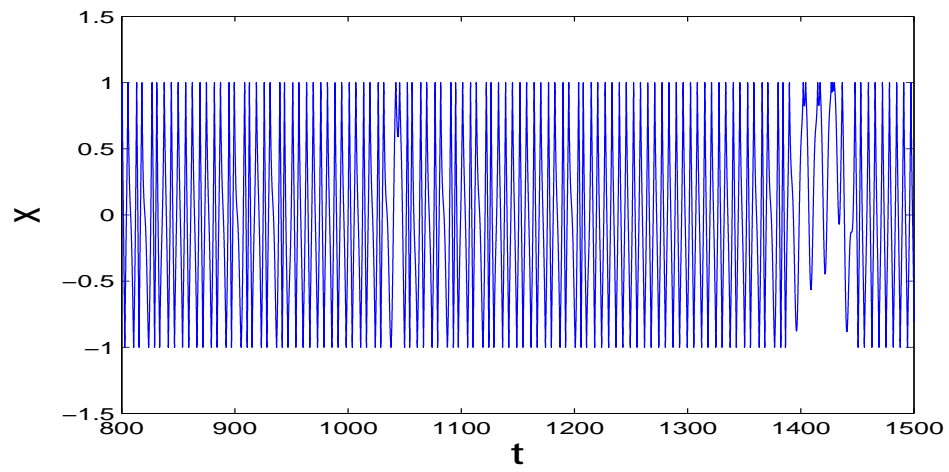


Figure 4.2: Displacement response in deterministic case.

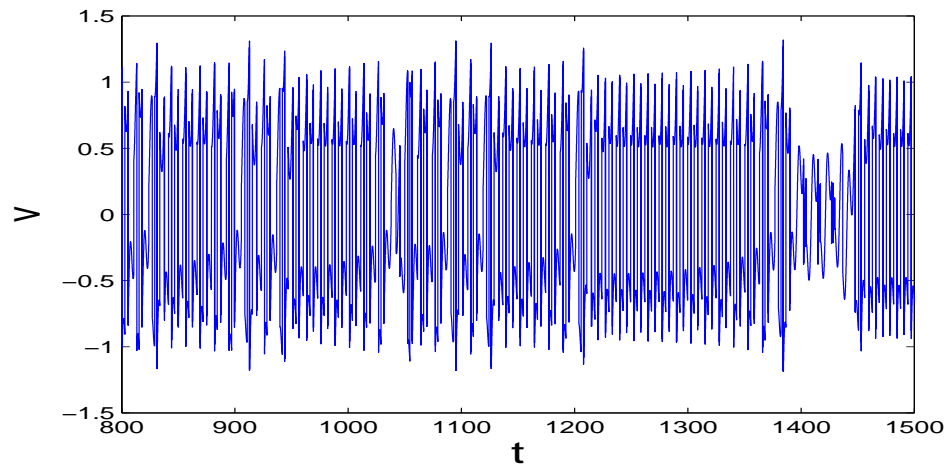


Figure 4.3: Velocity response in deterministic case.

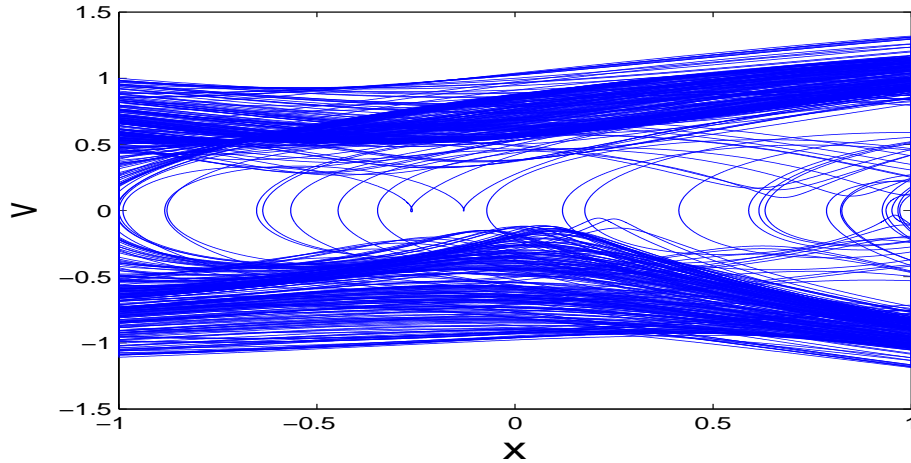


Figure 4.4: Phase plot.

Monte Carlo simulation is adopted to verify the efficiency of path integration method by comparing the consistency of results between the two methods. Figures 4.5 and 4.6 represent the comparison results between Monte Carlo simulation and path integration on joint and marginal probability distributions. It can be seen that the results from path integration match well with that from Monte Carlo simulation, which could illustrate the high accuracy of path integration method on capturing the random response in rattling system.

The deterministic response at certain moment is a fixed value while the response of a system excited by random component diffuses within a certain scope, which could be represented by probability distribution. Figures 4.7 and 4.8 show the joint probability distribution at four different time instants with different restitution coefficients. Vibro-impact in two sides ($x = \pm 1$) and the evolution of joint probability distribution could be observed from Figs. 4.7 and 4.8. The abrupt change of velocity on amplitude and direction occurs at the impact moment.

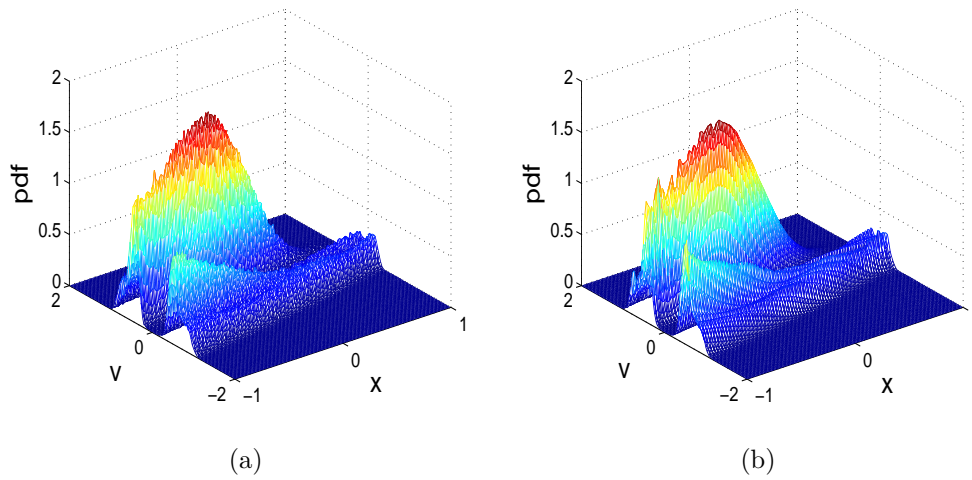


Figure 4.5: Joint distribution ($s = 0.9$, $t = 188.496$). (a) Monte Carlo simulation; (b) path integration.

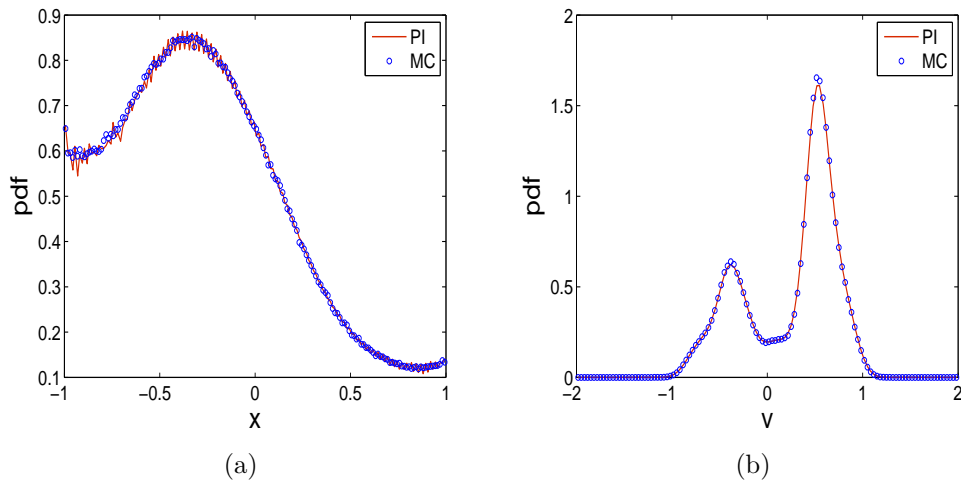


Figure 4.6: Marginal distribution ($s = 0.9$, $t = 188.496$). (a) displacement; (b) velocity.

Figure 4.9 compares the influence of different Gaussian white noise intensities on joint probability distribution. The main difference between Figs. 4.9 (a) and 4.9 (b) comes from the peak height. Stronger white noise means stronger perturbation, which could directly lead to wider probability distribution and lower peaks.

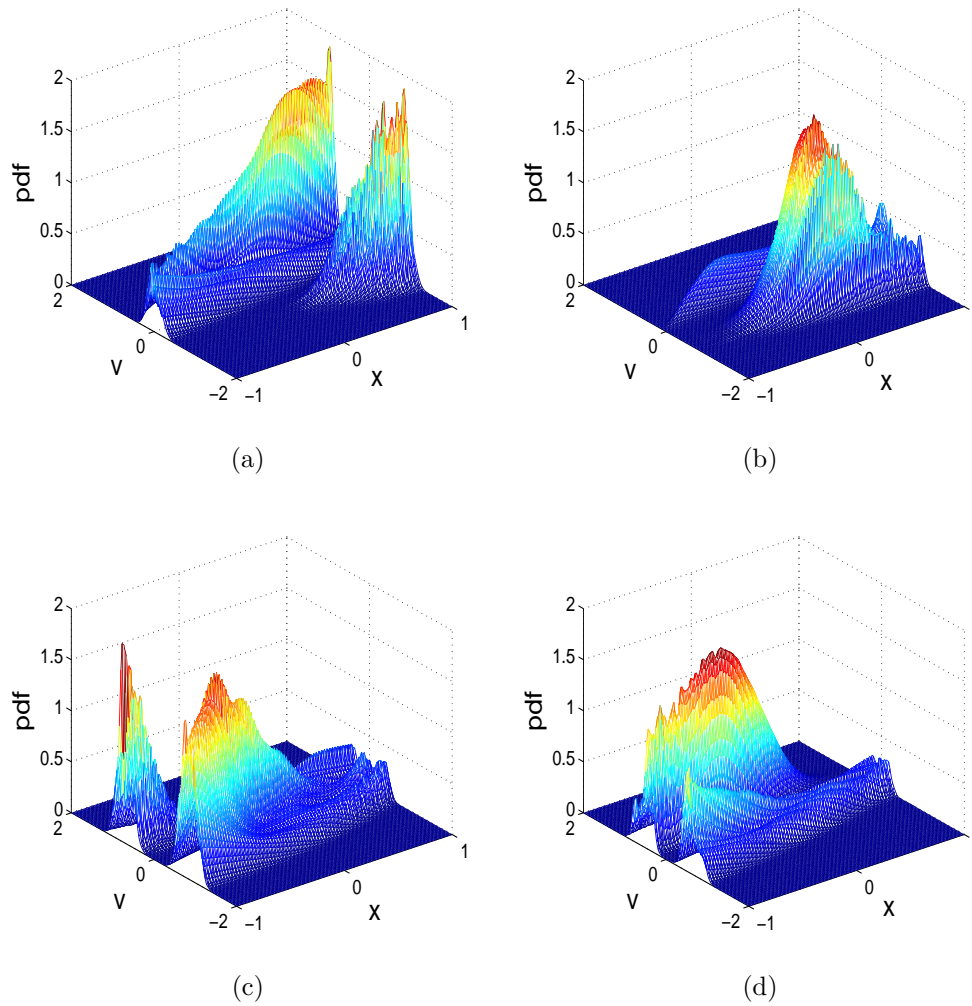


Figure 4.7: Surface plot of probability distribution ($s = 0.9$). (a) $t = 246.615$; (b) $t = 248.186$; (c) $t = 249.757$; (d) $t = 251.327$.

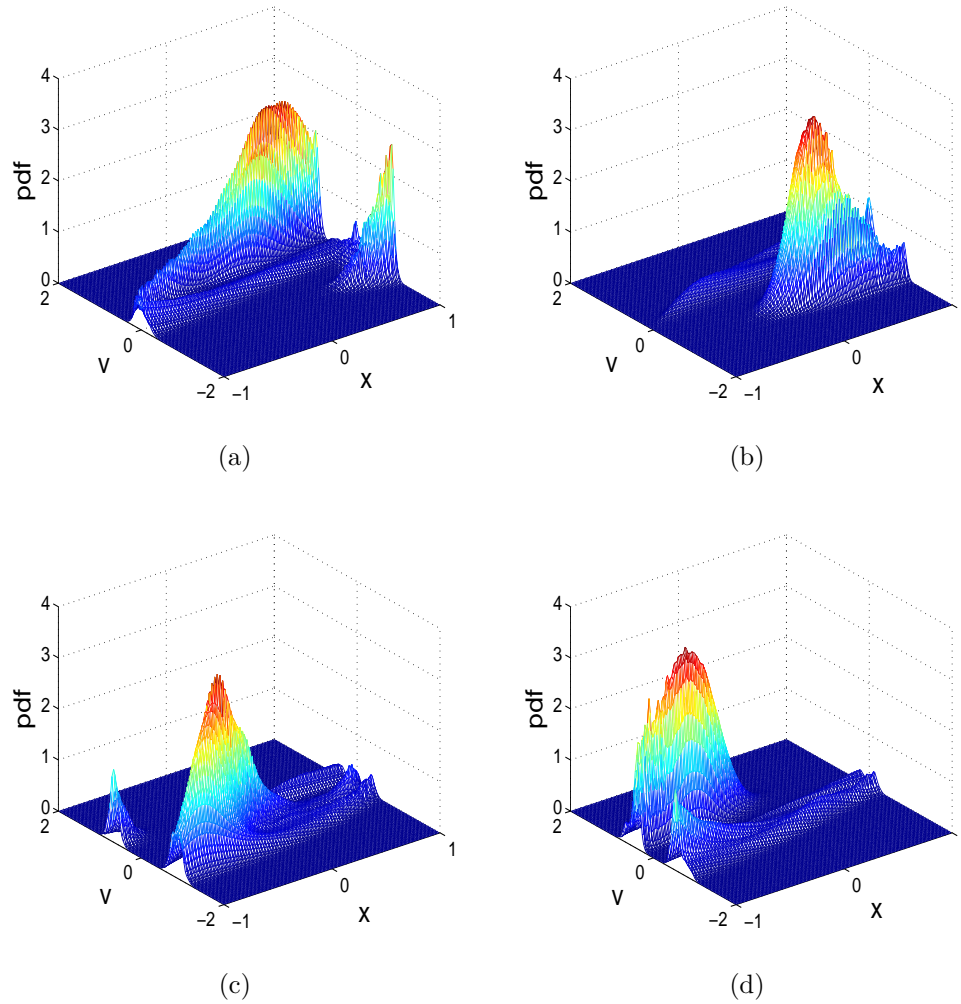


Figure 4.8: Surface plot of probability distribution ($s = 0.8$). (a) $t = 246.615$; (b) $t = 248.186$; (c) $t = 249.757$; (d) $t = 251.327$.

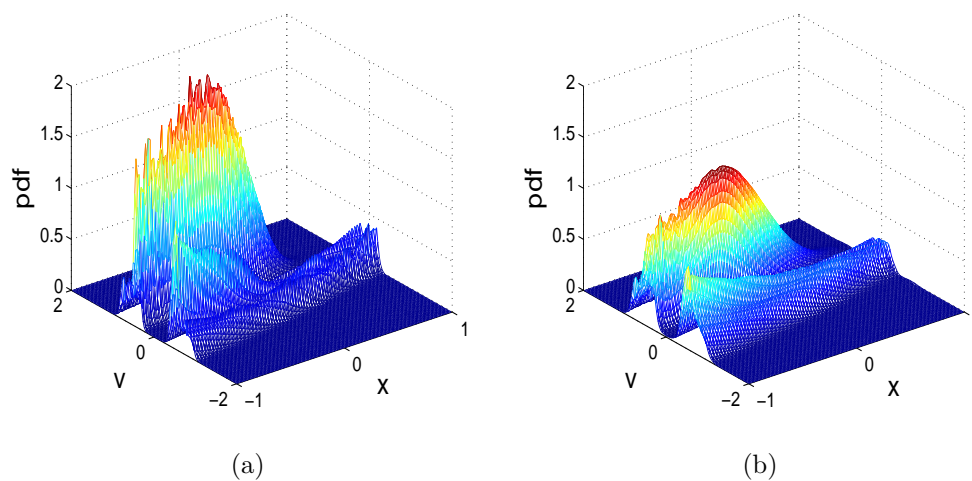


Figure 4.9: Joint probability distribution with different white noise intensities ($s = 0.9$, $t = 251.327$). (a) $r = 0.0025$; (b) $r = 0.0075$.

4.5 Conclusions

The random response of a single stage gear rattling model has been investigated by path integration method for the first time. A degenerate multidimensional transition PDF is applied. The probability distributions with different restitution coefficients at four time instants are presented. The aperiodicity of the response has been studied in deterministic case. The consistency between results from Monte Carlo simulation and path integration indicates the successful application of path integration method in the random dynamics study of gear rattling system.

Chapter 5

Conclusions and Future Work

5.1 Conclusions

The random response of a spur gear pair has been investigated by path integration method. Different path integration approaches are adopted based on the form of transition PDF and approach to obtain its mean and variance. Chapter 2 presents a two-dimensional Gaussian transition PDF and its parameters are calculated by moment equations. The same form of transition PDF is adopted in Chapter 3 while a new approach to obtain the variance is proposed. The method applied in Chapter 2 is limited to single-sided impact in gear dynamics, while the method presented in Chapter 3 could be applied to no impact, single-sided impact and double-sided impact. A degenerate multidimensional transition PDF is applied to deal with the gear rattling problem in Chapter 4.

The random response of a spur gear pair is represented as the joint probability distribution of displacement and velocity. For comparison purposes, deterministic response is also investigated. The multiple coexisting stable motions are captured in determin-

istic and random cases in Chapter 3. In random case, the multiple coexisting stable motions are displayed with multiple peaks in joint probability distribution. The application of path integration method in gear rattling system is pioneering. Based on the good agreement between the results from deterministic case, path integration and Monte Carlo simulation, the application of path integration method in the study of random response of a spur gear pair is successful and effective.

5.2 Future Work

Based on the present work, future work could be extended to the following aspects:

- The method presented in Chapter 2 is used to investigate the random response of a spur gear pair in single-sided impact case. In the case of no impact, the system is actually more simple with the elimination of the backlash nonlinearity. And such a system could be studied with the same method presented in Chapter 2 without the procedure of curve fitting.
- The study of nonlinear gear dynamics revealed complicated dynamic phenomena, like multiple coexisting stable motions and chaotic motions [6, 9, 16]. The multiple coexisting stable motions in random case have been captured in Chapter 3. Mo and Naess [32] investigated the chaotic motion of a stochastic spur gear pair model with backlash, but the chaos study of a more realistic stochastic gear model which also considers the time-varying mesh stiffness could be conducted with the method proposed in Chapter 3 in future work.
- The current stochastic gear model is based on a single stage. Yang [30] has extended his stochastic gear dynamics study to two-stage gears. The stochastic gear dynamics study could be extended to multi-stage gears in future. In

that case, the system is more complicated due to the increase of the degree of freedom. Besides, as mentioned by Kahraman and Singh [9], the harmonic excitation derives from both internal and external aspects. Current gear models in Chapters 2 and 3 consider only harmonic excitation from the internal aspect. The harmonic excitation in the later stochastic gear model could include multiple harmonics from both internal and external aspects.

Bibliography and References

- [1] W. A. Tuplin, “Gear-tooth stresses at high speed,” *Proceedings of the Institution of Mechanical Engineers*, vol. 163, no. 1, pp. 162–175, 1950.
- [2] W. A. Tuplin, “Dynamic load on gear teeth,” *Machine Design*, vol. 25, pp. 203–211, 1953.
- [3] H. Nevzat Özgüven and D. R. Houser, “Mathematical models used in gear dynamics—a review,” *Journal of Sound and Vibration*, vol. 121, no. 3, pp. 383–411, 1988.
- [4] T. Nakada and M. Utagawa, “The dynamic loads on gear caused by the varying elasticity of the mating teeth,” in *Proceedings of the 6th Japan National Congress for Applied Mechanics*, pp. 493–497, 1956.
- [5] S. L. Harris, “Dynamic loads on the teeth of spur gears,” *Proceedings of the Institution of Mechanical Engineers*, vol. 172, no. 1, pp. 87–112, 1958.
- [6] A. Kahraman and G. Blankenship, “Experiments on nonlinear dynamic behavior of an oscillator with clearance and periodically time-varying parameters,” *Journal of Applied Mechanics*, vol. 64, no. 1, pp. 217–226, 1997.
- [7] J. Wang, R. Li, and X. Peng, “Survey of nonlinear vibration of gear transmission systems,” *ASME Applied Mechanics Review*, vol. 56, pp. 309–330, 2003.

- [8] R. Comparin and R. Singh, “Non-linear frequency response characteristics of an impact pair,” *Journal of sound and vibration*, vol. 134, no. 2, pp. 259–290, 1989.
- [9] A. Kahraman and R. Singh, “Non-linear dynamics of a spur gear pair,” *Journal of sound and vibration*, vol. 142, no. 1, pp. 49–75, 1990.
- [10] A. Kahraman and R. Singh, “Interactions between time-varying mesh stiffness and clearance non-linearities in a geared system,” *Journal of Sound and Vibration*, vol. 146, no. 1, pp. 135–156, 1991.
- [11] K. Karagiannis and F. Pfeiffer, “Theoretical and experimental investigations of gear-rattling,” *Nonlinear Dynamics*, vol. 2, no. 5, pp. 367–387, 1991.
- [12] G. Blankenship and A. Kahraman, “Steady state forced response of a mechanical oscillator with combined parametric excitation and clearance type non-linearity,” *Journal of Sound and Vibration*, vol. 185, no. 5, pp. 743–765, 1995.
- [13] A. Kahraman and G. Blankenship, “Interactions between commensurate parametric and forcing excitations in a system with clearance,” *Journal of Sound and Vibration*, vol. 194, no. 3, pp. 317–336, 1996.
- [14] H. Moradi and H. Salarieh, “Analysis of nonlinear oscillations in spur gear pairs with approximated modelling of backlash nonlinearity,” *Mechanism and Machine Theory*, vol. 51, pp. 14–31, 2012.
- [15] S. Natsiavas, S. Theodossiades, and I. Goudas, “Dynamic analysis of piecewise linear oscillators with time periodic coefficients,” *International Journal of Non-Linear Mechanics*, vol. 35, no. 1, pp. 53–68, 2000.

- [16] S. Theodossiades and S. Natsisvas, “Non-linear dynamics of gear-pair systems with periodic stiffness and backlash,” *Journal of Sound and Vibration*, vol. 229, pp. 287–310, 2000.
- [17] R. Parker, S. Vijayakar, and T. Imajo, “Non-linear dynamic response of a spur gear pair: modelling and experimental comparisons,” *Journal of Sound and vibration*, vol. 237, no. 3, pp. 435–455, 2000.
- [18] R. G. Munro, *The dynamic behaviour of spur gears*. PhD thesis, University of Cambridge., 1962.
- [19] D. V. Iourtchenko, E. Mo, and A. Naess, “Response probability density functions of strongly non-linear systems by the path integration method,” *International Journal of Non-Linear Mechanics*, vol. 41, no. 5, pp. 693–705, 2006.
- [20] J. S. Yu and Y. K. Lin, “Numerical path integration of a non-homogeneous markov process,” *International Journal of Non-Linear Mechanics*, vol. 39, pp. 1493–1500, 2004.
- [21] A. Naess and V. Moe, “Efficient path integration methods for nonlinear dynamic systems,” *Probabilistic engineering mechanics*, vol. 15, no. 2, pp. 221–231, 2000.
- [22] J. Q. Sun and C. S. Hsu, “The generalized cell mapping method in nonlinear random vibration based upon short-time gaussian approximation,” *ASME:Journal of Applied Mechanics*, vol. 57, pp. 1018–1025, 1990.
- [23] A. Naess, F. E. Kolnes, and E. Mo, “Stochastic spur gear dynamics by numerical path integration,” *Journal of Sound and Vibration*, vol. 302, pp. 936–950, 2007.
- [24] H. Herzel, *The Fokker-Planck-Equation: Methods of Solution and Applications*. Springer-Verlag, 1989.

- [25] J. S. Yu, G. Q. Cai, and Y. K. Lin, “A new path integration procedure based on gauss-legendre scheme,” *International Journal of Non-Linear Mechanics*, vol. 32, pp. 759–768, 1997.
- [26] C. Soize, *The Fokker-Planck equation for stochastic dynamical systems and its explicit steady state solutions*, vol. 17. World Scientific, 1994.
- [27] F. Pfeiffer and A. Kunert, “Rattling models from deterministic to stochastic processes,” *Nonlinear Dynamics*, vol. 1, no. 1, pp. 63–74, 1990.
- [28] Y. Wang and W. J. Zhang, “Stochastic vibration model of gear transmission systems considering speed-dependent random errors,” *Nonlinear Dynamics*, vol. 17, pp. 187–203, 1998.
- [29] J. Yang and P. Yang, “Random gear dynamics based on path integration method,” in *ASME 2012 International Mechanical Engineering Congress and Exposition*, pp. 879–887, American Society of Mechanical Engineers, 2012.
- [30] J. Yang, “Vibration analysis on multi-mesh gear-trains under combined deterministic and random excitations,” *Mechanism and Machine Theory*, vol. 59, pp. 20–33, 2013.
- [31] A. Kunert and F. Pfeiffer, “Stochastic model for rattling in gear-boxes,” *Nonlinear Dynamics in Engineering Systems*, pp. 173–180, 1990.
- [32] E. Mo and A. Naess, “Nonsmooth dynamics by path integration: An example of stochastic and chaotic response of a meshing gear pair,” *ASME: Journal of Computational and Nonlinear Dynamics*, vol. 4, p. 034501, 2009.

- [33] J. Wang and I. Howard, “The torsional stiffness of involute spur gears,” *Proceedings of the Institution of Mechanical Engineers, Part C: Journal of Mechanical Engineering Science*, vol. 218, pp. 131–142, 2004.
- [34] T. Kiekbusch, D. Sappok, B. Sauer, and I. Howard, “Calculation of the combined torsional mesh stiffness of spur gears with two- and three-dimensional parametrical fe models,” *Strojniški vestnik-Journal of Mechanical Engineering*, vol. 57, pp. 810–818, 2011.
- [35] L. D. Lutes and S. Sarkani, *Random vibrations: analysis of structural and mechanical systems*. Butterworth-Heinemann, 2004.
- [36] A. Naess and J. M. Johnsen, “Response statistics of nonlinear dynamic systems by path integration,” in *Nonlinear Stochastic Mechanics*, pp. 401–414, Springer, 1992.
- [37] A. Naess and J. Johnsen, “Response statistics of nonlinear, compliant offshore structures by the path integral solution method,” *Probabilistic Engineering Mechanics*, vol. 8, no. 2, pp. 91–106, 1993.
- [38] Q. Feng and F. Pfeiffer, “Stochastic model on a rattling system,” *Journal of Sound and Vibration*, vol. 215, no. 3, pp. 439–453, 1998.

Appendices

For the system

$$\ddot{u} + \alpha\dot{u} = f(t) \quad (5.1)$$

$$f(t) = f_0 + f_1 \cos(\Omega_m t) + \xi(t) \quad (5.2)$$

The impulse response function for u

$$h_u(t) = \alpha^{-1}(1 - e^{-\alpha t}) \quad (5.3)$$

The autocorrelation function for $f(t)$

$$\begin{aligned} \phi_{ff} &= E[f(t)f(s)] = E[(f_0 + f_1 \cos(\Omega_m t) + \xi(t))(f_0 + f_1 \cos(\Omega_m s) + \xi(s))] \\ &= E[f_0^2 + f_0 f_1 (\cos(\Omega_m s) + \cos(\Omega_m t)) + f_0 \xi(s) + f_1^2 \cos(\Omega_m t) \cos(\Omega_m s) \\ &\quad + f_1 \cos(\Omega_m t) \xi(s) + \xi(t)(f_0 + f_1 \cos(\Omega_m s) + \xi(s))] \\ &= f_0^2 + f_0 f_1 (\cos(\Omega_m s) + \cos(\Omega_m t)) + f_1^2 \cos(\Omega_m t) \cos(\Omega_m s) + G_0 \delta(t - s) \end{aligned} \quad (5.4)$$

The autocovariance function for $f(t)$

$$\begin{aligned}
K_{ff} &= \phi_{ff} - E[f(t)] E[f(s)] \\
&= f_0^2 + f_0 f_1 (\cos(\Omega_m s) + \cos(\Omega_m t)) + f_1^2 \cos(\Omega_m t) \cos(\Omega_m s) \\
&\quad + G_0 \delta(t - s) - (f_0 + f_1 \cos(\Omega_m t))(f_0 + f_1 \cos(\Omega_m s)) \\
&= G_0 \delta(t - s)
\end{aligned} \tag{5.5}$$

The autocovariance function for displacement u

$$\begin{aligned}
K_{uu}(t_1, t_2) &= \int_{-\infty}^{\infty} \int_{-\infty}^{\infty} K_{ff}(s_1, s_2) h_u(t_1 - s_1) h_u(t_2 - s_2) ds_1 ds_2 \\
&= \frac{G_0}{\alpha^2} \int_{-\infty}^{\infty} \int_{-\infty}^{\infty} \delta(s_1 - s_2) (1 - e^{-\alpha(t_1 - s_1)}) (1 - e^{-\alpha(t_2 - s_2)}) ds_1 ds_2 \\
&= \frac{G_0}{\alpha^2} \int_0^{\min(t_1, t_2)} (1 - e^{-\alpha(t_1 - s)}) (1 - e^{-\alpha(t_2 - s)}) ds \\
&= \frac{G_0}{\alpha^2} \int_0^{\min(t_1, t_2)} (1 - e^{-\alpha(t_1 - s)} - e^{-\alpha(t_2 - s)} + e^{-\alpha(t_1 + t_2 - 2s)}) ds \\
&= \frac{G_0}{\alpha^2} \left(s - \frac{1}{\alpha} e^{-\alpha(t_1 - s)} - \frac{1}{\alpha} e^{-\alpha(t_2 - s)} + \frac{1}{2\alpha} e^{-\alpha(t_1 + t_2 - 2s)} \right) \Big|_0^{\min(t_1, t_2)}
\end{aligned} \tag{5.6}$$

when $t_1 = t_2$

$$\sigma_1^2 = \frac{G_0}{\alpha^2} \left[t - \frac{1}{\alpha} \left(\frac{3}{2} - 2e^{-\alpha t} + \frac{1}{2} e^{-2\alpha t} \right) \right] \tag{5.7}$$

The impulse response function for \dot{u}

$$h_{\dot{u}}(t) = e^{-\alpha t} \tag{5.8}$$

The autocovariance function for velocity \dot{u}

$$\begin{aligned}
K_{\dot{u}\dot{u}}(t_1, t_2) &= \int_{-\infty}^{\infty} \int_{-\infty}^{\infty} K_{ff}(s_1 - s_2) h_{\dot{u}}(t_1 - s_1) h_{\dot{u}}(t_2 - s_2) ds_1 ds_2 \\
&= G_0 \int_0^{\min(t_1, t_2)} e^{-\alpha(t_1+t_2-2s)} ds \\
&= G_0 \left(\frac{1}{2\alpha} e^{-\alpha(t_1+t_2-2s)} \right) \Big|_0^{\min(t_1, t_2)} \tag{5.9}
\end{aligned}$$

when $t_1 = t_2$

$$\sigma_2^2 = \frac{G_0}{2\alpha} (1 - e^{-2\alpha t}) \tag{5.10}$$

The cross-covariance function for displacement u and velocity \dot{u}

$$\begin{aligned}
K_{u\dot{u}}(t_1, t_2) &= \int_{-\infty}^{\infty} \int_{-\infty}^{\infty} K_{ff}(s_1, s_2) h_u(t_1 - s_1) h_{\dot{u}}(t_2 - s_2) ds_1 ds_2 \\
&= \int_{-\infty}^{\infty} \int_{-\infty}^{\infty} G_0 \delta(s_1 - s_2) \alpha^{-1} (1 - e^{-\alpha(t_1-s_1)}) e^{-\alpha(t_2-s_2)} ds_1 ds_2 \\
&= \frac{G_0}{\alpha} \int_0^{\min(t_1, t_2)} (e^{-\alpha(t_2-s)} - e^{-\alpha(t_1+t_2-2s)}) ds \\
&= \frac{G_0}{\alpha} \left(\frac{1}{\alpha} e^{-\alpha(t_2-s)} - \frac{1}{2\alpha} e^{-\alpha(t_1+t_2-2s)} \right) \Big|_0^{\min(t_1, t_2)} \tag{5.11}
\end{aligned}$$

when $t_1 = t_2$

$$\begin{aligned}
\sigma_{12} &= \frac{G_0}{\alpha} \left(\frac{1}{\alpha} (1 - e^{-\alpha t}) - \frac{1}{2\alpha} (1 - e^{-2\alpha t}) \right) \\
&= \frac{G_0}{\alpha^2} \left[1 - e^{-\alpha t} - \frac{1}{2} + \frac{1}{2} e^{-2\alpha t} \right] \\
&= \frac{G_0}{\alpha^2} \left[\frac{1}{2} - e^{-\alpha t} + \frac{1}{2} e^{-2\alpha t} \right] \tag{5.12}
\end{aligned}$$